

UNIVERZA V LJUBLJANI
FAKULTETA ZA FARMACIJO

MAJA ANA STRNAD

MAGISTRSKA NALOGA

MAGISTRSKI ŠTUDIJSKI PROGRAM INDUSTRIJSKA
FARMACIJA

Ljubljana, 2017

UNIVERSITY OF LJUBLJANA

FACULTY OF PHARMACY

MAJA ANA STRNAD

**VREDNOTENJE FOTO-FIZIKALNIH LASTNOSTI IZBRANEGA
SILIL-KSANTENSKEGA DERIVATA, FLUORESCENČNEGA
OZNAČEVALCA ŽIVIH CELIC**

**EVALUATION OF PHOTO-PHYSICAL PROPERTIES OF
SELECTED LIVE-CELL-MARKER, SILYL-XANTHENE
DERIVATIVE**

MASTER'S STUDY PROGRAMME INDUSTRIAL PHARMACY

Ljubljana, 2017

The experimental work for this Master's thesis was conducted from March 2016 until June 2016 at the Department of Physical Chemistry at the Faculty of Pharmacy in Granada, Spain, under the supervision of prof. dr. José Manuel Paredes Martínez.

Acknowledgments

I would like to express my sincere gratitude to prof. dr. Anamarija Zega for her advice on my Master's thesis and her willingness to assist me to a great extent.

I am extremely grateful to prof. dr. José Manuel Paredes Martínez for his kindness, patience, professional advice on my experimental work and all his efforts to make my stay in Granada a really beautiful and memorable experience. Exceptional acknowledgment goes to him as well as prof. dr. José María Álvarez Pez, who warmly included me in his research group. Great thanks to all the remaining staff at the laboratory, who have also contributed greatly to the development of my research work.

I would also like to express my appreciation to Virginia for all her support and encouragement. She will always be my great role model and a true friend, who blessed me with her pleasant company and a willingness to assist whenever I needed.

My deepest gratitude goes to my family for supporting me during my studies and overall in my life.

And finally, big thanks to all my closest friends, who have accompanied me in the recent years and shared these unforgettable years of studies with me.

Statement

I hereby declare that this Master's thesis was done independently by me under mentorship of assoc. prof. dr. Anamarija Zega, MSc. pharm. and co-mentorship of prof. dr. José Manuel Paredes Martínez.

Maja Ana Strnad

Commission president: assoc. prof. dr. Robert Roškar

Commission member: dr. Ilija Ilić

Ljubljana, 2017

TABLE OF CONTENTS

ABSTRACT	V
EXTENDED ABSTRACT IN SLOVENE	VI
LIST OF ABBREVIATIONS	IX
LIST OF FIGURES	X
LIST OF TABLES	XI
1 INTRODUCTION.....	1
1.1 UV/VIS absorption spectroscopy	1
1.1.1 Beer-Lambert law	2
1.1.2 Absorption spectra	3
1.1.3 Isosbestic point	4
1.1.4 UV/VIS spectrophotometer	5
1.2 Fluorescence spectroscopy	6
1.2.1 Phenomena of fluorescence	6
1.2.2 Jablonski diagram	7
1.2.3 Fluorescent labelling	8
1.2.3.1 Fluorescein	10
1.2.3.2 ESPT reaction.....	11
1.2.4 Spectrofluorometers.....	13
1.2.5 Time-resolved emission spectroscopy (TRES)	14
1.3 Fluorescence lifetime imaging microscopy (FLIM).....	14
2 RESEARCH AIM AND OBJECTIVES	16
3 MATERIALS AND METHODS	17
3.1 Materials	17

3.1.1	Reagents	17
3.1.2	Laboratory equipment.....	18
3.1.3	Instrumentation.....	19
3.2	Methods	19
3.2.1	Preparation of stock dye solution	20
3.2.2	Preparation of phosphate buffer solutions	20
3.2.3	Preparation of solutions for the measurements	21
3.2.3.1	Solutions for the pK _a calculation.....	21
3.2.3.2	Solutions for the TRES experiments.....	21
3.2.3.3	Solutions for the FLIM experiments - in DMEM	22
3.2.3.4	Solutions for the FLIM experiments - the HEK 293 cells	22
3.2.4	Measuring the absorbance with the UV-VIS spectrophotometer.....	22
3.2.5	Measuring the fluorescence with a fluorescence spectrophotometer	23
3.2.6	Measuring with time-resolved fluorometer	24
3.2.7	Measuring with inverse time-resolved confocal fluorescence microscope ...	25
3.3	Evaluation of the measurements	26
3.3.1	Analysis of the experimental absorbance versus pH used to determine the ground-state equilibrium of 2-Me-4OMe-TM.....	27
3.3.2	Analysis of the experimental fluorescence versus pH used to determine the ground-state equilibrium of 2-Me-4OMe-TM.....	28
3.3.3	Evaluation of kinetic parameters from the lifetimes at high phosphate buffer concentrations.....	28
4	RESULTS AND DISCUSSION	30
4.1	General findings.....	30
4.2	Absorption measurements and ground-state equilibria.....	30
4.3	Steady-state emission spectra	33
4.3.1	Produced ESPT reaction.....	35

4.4	TRES.....	36
4.5	Kinetic and spectral parameters of the ESPT reaction	38
4.6	FLIM.....	40
4.6.1	FLIM - biomimetic media DMEM.....	40
4.6.2	FLIM - HEK 293 cells.....	42
5	CONCLUSION.....	45
6	REFERENCES.....	47

ABSTRACT

Fluorescein is the well-known xanthene molecule and remains one of the most widely used fluorophores. Analytical methods, such as fluorescent imaging and spectroscopy operate with it because of its high molar absorptivity and high quantum yield. It has a versatile core that can be modified further to tune properties such as acidity constant (pK_a) or excitation and/or emission wavelengths. Therefore, a wide repertoire of fluorescein derived molecules with certain chemical groups attached that are extensively used as tools for cellular biology studies already exists.

The context of this master's thesis **was to evaluate the photo-physical properties** of the new silyl-xanthene type compound. That being the case, the recently synthesized compound, **2-Me-4OMe-TM**, was the red thread of our studies. During the experimental part of the thesis, the analyte with clinical potential application was selected: phosphate ions. We prepared a series of sample solutions with our compound and recorded their absorption and emission spectra. We also determined the value of the pK_a and pK_a in excited-state (pK_a^*). We checked if the phosphate buffer-mediated excited-state proton transfer reaction (ESPT) occurs between the anionic and neutral forms of **2-Me-4OMe-TM** at different pH values (performing emission spectroscopy in steady-state and time-resolved spectroscopy). The kinetic and spectral parameters of the phosphate-mediated ESPT reaction were obtained. Due to the presence of the ESPT reaction, we evaluated the ability of the **2-Me-4OMe-TM** dye to estimate the concentration of appropriate proton donor/acceptor in samples, therefore simulating the intracellular environment, and inside cell lines (with fluorescence lifetime imaging microscopy - FLIM).

The absorption and emission spectra at steady-state showed two spectroscopically distinguishable species (anion and neutral form) which converted into each other as the pH varied, and gave rise to the formation of one noticed isosbestic point. The pK_a of the dye at near-neutral pH were 7.3 and 7.8. ESPT reaction was produced between the neutral and the anion species of our compound. The value of the pK_a^* was 6.56. We concluded that our derivative could be used as a real-time phosphate intracellular sensor in cultured cells because of its solid penetration into cells.

Key words: photo-physical properties, phosphate ions, ESPT reaction, real-time phosphate intracellular sensor, cultured cells

EXTENDED ABSTRACT IN SLOVENE

Razširjen povzetek v slovenskem jeziku

Osnova spektroskopskih analiznih metod je merjenje elektromagnetnega valovanja, ki povzroči interakcije med molekulami v vzorcu, da ga le-te absorbirajo ali emitirajo. Spektroskopske metode so razdeljene na absorpcijske in emisijske, če opazujemo pojav, če pa opazujemo samo naravo snovi, jih razdelimo na atomsko in molekularno spektroskopijo. Zaradi svoje visoke občutljivosti so med najpomembnejšimi metodami v kemijski analizi.

Molekule imajo več energijskih nivojev, pravimo, da zasedajo različna energijska stanja. Osnovno stanje molekule je ravnovesno stanje in tu molekula zaseda najnižja energijska oz. elektronska stanja. Ko pa molekulo obsevamo s primernim elektromagnetnim valovanjem, preide v energijsko višji nivo. Poleg elektronskih stanj imajo molekule še vibracijska in rotacijska stanja. Eden od načinov relaksacije molekule nazaj v osnovno ravnovesno stanje je v obliki fluorescence, pri čemer molekula odda foton.

Fluorofor je kemijska spojina, ki absorbira svetlobno energijo določene valovne dolžine in jo nato odda pri daljši valovni dolžini v obliki fluorescence. Da snov fluorescira, mora molekula vsebovati določene strukturne fragmente. Fluorofori običajno vsebujejo več kondenziranih aromatskih sistemov ali konjugiranih dvojnih vezi, na fluorescenco pa vplivajo tudi vse funkcionalne skupine, ki lahko z resonančnimi in induktivnimi vplivi spremenijo elektronsko gostoto (polarnost) osnovnega sistema. Običajno proteini ali druge ključne biomolekule ne izkazujejo intrinzične fluorescence, ki je potrebna za specifično identifikacijo. Če molekula/makromolekula, ki jo želimo opazovati, ne fluorescira, jo označimo tako, da ji pripnemo fluorofor. Fluorescentni označevalec se specifično veže na preiskovano biološko molekulo (DNA ali protein) ali se lokalizira v določeni celični regiji na podlagi kovalentnih, elektrostatskih ali hidrofobnih interakcij. Obstajajo še fluorofori, ki se uporabljajo za sledenje dinamičnih procesov in lokaliziranih sprememb, kot so: koncentracije kovinskih ionov, reaktivnih kisikovih spojin in sprememba membranskega potenciala. Fluorofori morajo biti čimbolj fotostabilni, imeti visok kvantni izkoristek in velik molarni ekstinkcijski koeficient.

Dobro znan fluorofor je fluorescein in ostaja eden najbolj uporabljenih fluoroforov za označevanje tkiv, celic ali materialov v sodobnih biokemijskih in bioloških raziskavah. Del njegove strukture, ki je odgovoren za fluorescenco, je ksantenski obroč in se nadalje lahko prilagaja lastnostim, kot so pK_a (konstanta kislinsko-bazičnega ravnotežja) ali valovnim dolžinam ekscitacije in/ali emisije. Z modifikacijo fluoresceina se je že razvil velik repertoar molekul, ki se v veliki meri uporabljajo kot orodja za študije celične biologije.

V okviru magistrske naloge smo ocenili fotofizikalne lastnosti novo sintetizirane spojine silil-ksantenskega tipa **2-Me-4OMe-TM**, ki fluorescira v odvisnosti od pH. Atom kisika na položaju 10 na ksantenskem obroču so nadomestili z atomom silicija (Si). Ta spojina je bila razvita z namenom uporabe v živih celicah, kot fluorescenčni označevalec, ki ohranja ključne prednosti matične strukture (fluoresceina). Naša spojina ima valovne dolžine absorpcijskih in emisijskih maksimumov približno 90 nm daljše od valovnih dolžin fluoresceina, pri čemer emitira svetlobo v vidnem območju elektromagnetnega sevanja.

Metode, ki smo jih uporabili v magistrski nalogi so UV-VIS spektroskopija, fluorescenčna spektroskopija, fluorescenčna spektroskopija s sistemom časovno koreliranega štetja posameznih fotonov (angl. time-correlated single photon counting - TCSPC) in konfokalna mikroskopija v kombinaciji s fluorescenčno mikroskopijo. V eksperimentalnem delu magistrske naloge smo izbrali analit s kliničnim potencialom: to so fosfatni ioni. Fosfatni anioni sodelujejo pri prenosu signala in shranjevanju energije v celicah in zunajceličnih medijih. Najprej smo pripravili vrsto vzorčnih raztopin fosfata, nato tudi naše spojine, in izvedli več meritev absorpcijskih in emisijskih spektrov.

Med samim postopkom priprave smo ugotovili, da je naša spojina občutljiva na svetlobo, zato je bilo pomembno, da smo našo spojino v pripravljene vzorce dodali neposredno pred vsako meritvijo. V prihodnje bi bilo ustrezno razmisliti, kako izboljšati fotostabilnost naše spojine, kot je ugodno za tovrstne fluorofore.

Naša želja je bila, da ima spojina največjo absorbanco pri pH v bližini fiziološkega pH celic (pH med 6,7 in 7,4), da bi bila primerna za označevanje le-teh. Glede na posnete absorpcijske spektre, naša spojina dobro absorbira v območju fiziološkega pH celic. V prisotnosti H^+ ionov (dodatek fosfatnega pufra) v bolj kislem okolju smo opazili spreminjanje oblike naše spojine, saj se je spremenilo ravnovesje med nevtralno in

anionsko obliko. V bližini nevtralnega pH ($\text{pH} \sim 7$) je bilo jasno vidno, da spojina prehaja iz nevtralne v ionizirano anionsko obliko in čedalje bolj fluorescira.

Z uporabo UV/VIS spektroskopije in fluorescenčne spektroskopije smo določili tudi vrednost $\text{p}K_a$ naše spojine v osnovnem stanju. Vrednost konstante nam pove, v kolikšni meri je spojina disociirala. Dobljeni vrednosti sta bili 7,3 in 7,8. V živih organizmih je kislinsko-bazično ravnotežje in sama kinetika odvisna od vrednosti $\text{p}K_a$ številnih kislin in baz, ki so prisotne v celicah teh organizmov. Zato na podlagi pridobljenih vrednosti $\text{p}K_a$ lahko sklepamo, da je naša spojina primerna za biološko uporabo pri nevtralnem pH, za označevanje bolj bazičnih bioloških sistemov.

Nadaljevali smo z vprašanjem, ali se lahko tvori reakcija prenosa protonov v vzbujenem stanju (angl. excited-state proton transfer reakcija - ESPT) med nevtralno in anionsko obliko naše spojine v vodnih raztopinah pri nevtralnem pH. V ta namen smo reakcijo vzpodbudili s primerno koncentracijo fosfatnega pufru. Reakcija je potekla. Zaradi obstoja te reakcije smo se lotili tudi izdelave emisijskih spektrov spojine pri nevtralnem pH, da bi videli kako se spojina obnaša v različnih časih po ekscitacijskem pulzu (angl. time resolved emission spectroscopy - TRES). Rezultati so pokazali, da je protonacija anionske oblike naše spojine glavni proces med samo reakcijo v vzbujenem stanju in poteka hitreje kot deprotonacija nevtralne oblike.

Ugotovljena je bila tudi vrednost konstante kislinsko-bazičnega ravnotežja v vzbujenem stanju in sicer $\text{p}K_a^* = 6,56$. Vrednost je nižja od tiste, ki smo jo dobili v ravnovesnem stanju, vendar še vedno v območju zanimivih $\text{p}K_a$ vrednosti za potencialno uporabo spojine v celicah pri nevtralnem pH.

Preverili smo tudi učinek različnih koncentracij fosfatnega pufru in naše spojine na življenjski čas fluorescence v mediju, ki posnema celično notranjost, in v celicah HEK 293, ki so bile gojene v fazi celične diferenciacije, s tehniko mikroskopiranja (angl. fluorescence lifetime imaging microscopy - FLIM). Prodor spojine v celice je bil lepo opazen in iz tega sklepamo, da bi našo spojino lahko uporabili kot intracelularni senzor fosfatnih ionov v celicah.

Ključne besede: UV/VIS in fluorescenčna spektroskopija, fluorescenčni označevalci, fotofizikalne lastnosti fluoroforov, fosfatni ioni, označevanje celic

LIST OF ABBREVIATIONS

BCECF	2',7'-bis(2-carboxyethyl)-5-(and-6)-carboxyfluorescein
CCD	charge-coupled device
CH	detection channel
DMEM	Dulbecco's modified Eagle medium
ESPT	excited state proton transfer reaction
FBS	foetal bovine serum
FCS	fluorescence correlation spectroscopy
FLIM	fluorescence lifetime imaging microscopy
IR	infrared spectroscopy
IRF	instrument response function
NADH	nicotinamide adenine dinucleotide, in a reduced form
MOU	main optical unit
NMR	nuclear magnetic resonance
PBS	phosphate-buffered saline
pK_a	acidity constant (ground-state)
pK_a^*	acidity constant for the excited-state
ROS	reactive oxygen species
SPAD	avalanche diodes
SPT	single-photon timing
TCSPC	time-correlated single photon counting
TRES	time-resolved emission spectroscopy
TTTR	time-tagged-time-resolved
UV	ultraviolet
VIS	visible

LIST OF FIGURES

Figure 1: Reducing the intensity of the beam of radiation due to absorption of the analyte in a solution, having a concentration c	2
Figure 2: Absorption spectra of 2-Me-4OMe-TM at different molar concentrations.	4
Figure 3: The spectra of basic (anion - A), neutral form (neutral - N), and a mix between both species (neutral and anion) are presented. All solutions have the same concentration of the analyte (10).	5
Figure 4: Scheme of UV/VIS spectrophotometer (13).	6
Figure 5: Stokes shift; the difference observed between both band maxima of the absorption and emission spectra of the same electronic transition.	7
Figure 6: Jablonski diagram (14).	8
Figure 7: Structures of typical fluorescent substances (14).	10
Figure 8: Fluorescein structure.	10
Figure 9: Four different prototropic forms of fluorescein: cation, neutral, monoanion and dianion (22).	11
Figure 10: Kinetic scheme of a compartmental system for both states of the ESPT reaction, which is promoted by an appropriate proton donor/acceptor (20).	12
Figure 11: Schematic representation of a spectrofluorometer.	13
Figure 12: FLIM image example. Fluorescence lifetimes are codified by colours, producing an image (20).	15
Figure 13: Fluorescent dye 2-Me-4OMe-TM and its two prototropic forms (A - anion, N - neutral, respectively).	18
Figure 14: Olympus IX71 inverted microscope scheme (33).	25
Figure 15: MOU scheme (20).	26
Figure 16: Absorption spectra of 7.94×10^{-6} M aqueous solutions of 2-Me-4OMe-TM in the pH range between 4.92 to 9.13.	31
Figure 17: Prototropic forms of 2-Me-4OMe-TM: A (anion), N (neutral).	32
Figure 18: Absorption spectra for the neutral (black) and anionic (red) form of 7.94×10^{-6} M aqueous solutions of 2-Me-4OMe-TM.	32
Figure 19: Recovered molar absorption coefficients versus wavelength for the neutral (blue) and anionic (pink) form of 2-Me-4OMe-TM.	33
Figure 20: Steady-state emission spectra of 2-Me-4OMe-TM.	34

Figure 21: Normalized fluorescence spectral profiles of the two prototropic forms of 2-Me-4OMe-TM: anion (black) and neutral (red).....	35
Figure 22: Steady-state emission spectra of 2-Me-4OMe-TM obtained for the calculation of pK_a^* value.	36
Figure 23: Normalized emission spectra observed at different times after the excitation pulse are shown (λ_{ex} 530 nm).....	37
Figure 24: Global fitting (solid lines) of the theoretical equations (eq. 13, 14, 15, 16) to the decay times at different buffer concentrations (0, 200, 400 and 700 mM) and pH values. Note the change in scale between the two sections of the ordinate axis.	39
Figure 25: Ground- and excited-state proton-transfer reactions represented by the kinetic model of aqueous 2-Me-4OMe-TM in phosphate buffer.	40
Figure 26: FLIM images of 1×10^{-7} M 2-Me-4OMe-TM in DMEM in 20 mM TRIS buffer, at pH 7.35 and with changing phosphate concentrations in the range of 0 to 300 mM (Pi).	41
Figure 27: Average decay time (dot) of 1×10^{-7} M 2-Me-4OMe-TM in DMEM in 20 mM TRIS buffer, at pH 7.35 and with changing phosphate concentrations in the range of 0 to 300 mM obtained from FLIM images and recovered lifetime (line) from the kinetic constants. Red - neutral, black - anion. Scale bars represent the standard deviation.	42
Figure 28: FLIM images of 4×10^{-7} M 2-Me-4OMe-TM in the cytoplasm of HEK 293 cells, treated with different phosphate concentrations.	43
Figure 29: Histograms of lifetimes recovered from Figure 28.	44
Figure 30: HEK 293 cells, treated with different concentrations of phosphate and the changes in the decay time of the fluorescence are presented in the graph. Average decay time (dot) and recovered lifetime (line).....	44

LIST OF TABLES

Table 1: 2-Me-4OMe-TM structure and the obtained photophysical parameters.	45
---	----

1 INTRODUCTION

The basis of spectroscopic analytical methods is to measure an interaction of the components in the sample under investigation with electromagnetic radiation. Due to their high sensitivity, several spectroscopic methods are amongst the most important methods in chemical analysis. Spectroscopic methods are divided into absorption and emission methods, if we observe the phenomenon, however if we observe the nature of the substance, we can divide them into atomic and molecular spectroscopy. If the substances in the sample (atoms, molecules) accept electromagnetic radiation, it is termed as absorption and if the substances give off some energy in the form of radiation, it is termed as emission (1).

1.1 UV/VIS absorption spectroscopy

UV/VIS spectroscopy is an analytical method widely used for the quantification of various inorganic and organic compounds and is based on the absorption of visible (with a wavelength between 340-800 nm) and ultraviolet light (180-340 nm). Atom, ion, or molecule can exist in a number of vibrational energy levels which may pass from the primary steady-state with a lower energy into unstable excited-state, with a higher energy. The part of the molecule responsible for the absorption of visible and UV light, is called chromophore or chromophore system (1, 2).

When we illuminate the cuvette that contains the sample with a monochromatic light (intensity I_0), the intensity of the transmitted light (I) will reduce due to the absorption of the substance in the solution (Figure 1) (1, 2). The sample absorbs light selectively. This is possible because the frequency of the selected light matches the electrons' frequency of the sample, therefore causing them to vibrate. In this case, the absorption is at its highest. Opposite of this, the reflection and transmission of light appear as a result of the mismatch between the frequencies of light and vibration of the sample (3). The transmittance (T) is the proportion of the transmitted light and is defined as a ratio between the intensity of the transmitted and incident light:

Equation 1

$$T = (I/I_0) \times 100$$

T - transmittance

I – intensity of the transmitted light

I_0 – intensity of monochromatic light

Absorbance (A) is defined by a logarithm of the correlation of incident to transmitted light through the sample:

Equation 2

$$A = -\log_{10} T$$

A – absorbance

T – transmittance

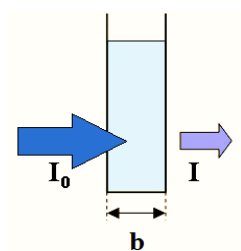


Figure 1: Reducing the intensity of the beam of radiation due to absorption of the analyte in a solution, having a concentration c .

Absorbance is dependent on the concentration of the analyte in the solution and also on the ray path length which travels through the solution, and independent of the intensity of the electromagnetic radiation (1, 2). A quantitative analysis of our compound can be carried out by means of UV/VIS spectroscopy. It is possible to check how well our compound will absorb UV or visible radiation.

1.1.1 Beer-Lambert law

Beer-Lambert law describes the relation between the concentration of the analyte and the absorbance. According to this law, the absorbance is directly corresponding to the path length (l), molar absorption coefficient (ϵ), which is typical for analyte, and the analyte concentration (c):

Equation 3

$$A = \epsilon \cdot c \cdot l$$

A – absorbance

ϵ – molar absorption coefficient [$\text{l} \cdot \text{mol}^{-1} \cdot \text{cm}^{-1}$]

c – analyte concentration [mol/l]

l – path length [cm]

The linearity of the Beer-Lambert law is limited by instrumental and chemical factors. Nonlinearity may come from:

- absorption coefficients at high concentrations deviating because of the electrostatic interactions between molecules placed close to each other,
- light scattering caused by the small particles in the sample,
- refractive index changing at high concentration of the analyte,
- chemical equilibria shifting due to dependence of the analyte concentration,
- non-monochromatic radiation (by applying a relatively flat part of the absorption spectra, the maximum of an absorption band for instance, deviations can be greatly reduced),
- stray light (1–5).

1.1.2 Absorption spectra

The absorption characteristics of the analyte are presented in an absorption spectra, which shows narrow peaks for simple molecules in the gaseous state, while the absorption spectra for ions and the molecules in solutions shows wider peaks. The latter are a result of a multitude of vibrational and rotational energy levels which are present in addition to the principal electronic transitions (2). Figure 2 shows an example of absorption spectra at different concentrations of the analyte.

The absorption spectra shows variation of intensity of the absorption as a function of wavelength. Wavelength of absorbed light depends on the distribution of atoms in the sample. Factors which can affect the absorption spectra are the environment of the molecule, pH and the polarity of the solvent. UV/VIS absorption spectra is insufficiently specific so we could not use it to determinate analyte identity (6).

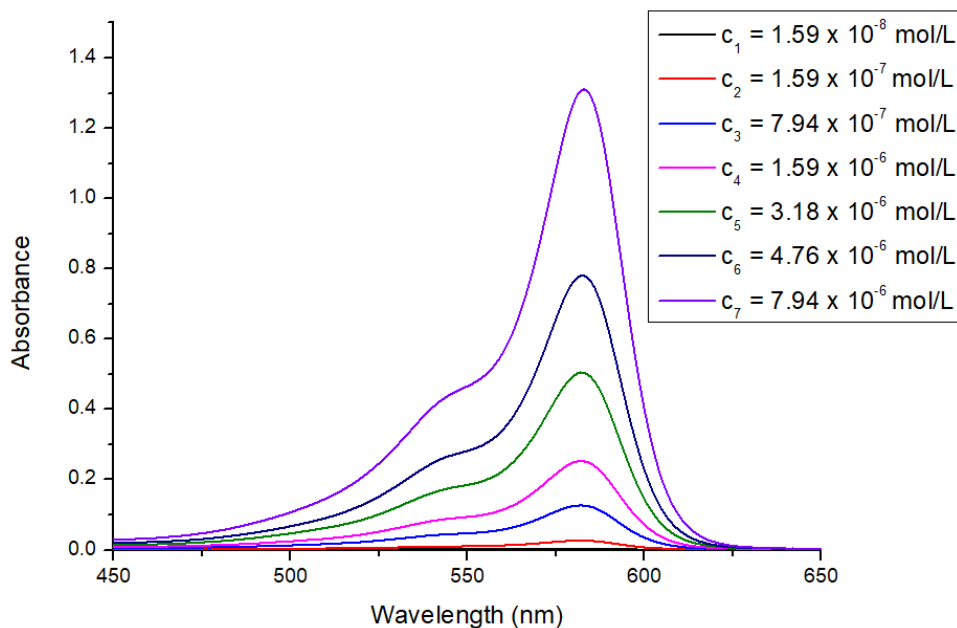


Figure 2: Absorption spectra of 2-Me-4OMe-TM at different molar concentrations.

1.1.3 Isosbestic point

An isosbestic point can be described as a point, where the total absorbance of a sample does not alter during a physical change of the sample or a chemical reaction. An isosbestic point represents a specific frequency, wavelength, or wavenumber (7, 8).

The isosbestic plot can be created from the superposition of the absorption spectra of two species (molar absorptivity can be used for the representation, or absorbance as a means to retain the same molar concentration for both species). In this case, the spectra cross each other and at the wavelength, where they are crossed, the isosbestic point is clearly seen (Figure 3). For a pair of substances more than one isosbestic points can be observed (8).

In chemical kinetics, where isosbestic points are often applied, they are used as reference points for the reaction rates studies (due to constant absorbance throughout the whole reaction at those wavelengths). In medicine, their use is a result of their success in determining hemoglobin concentration. And finally, they are used in clinical chemistry as a means to ensure quality by verifying the wavelength accuracy of a spectrophotometer (9).

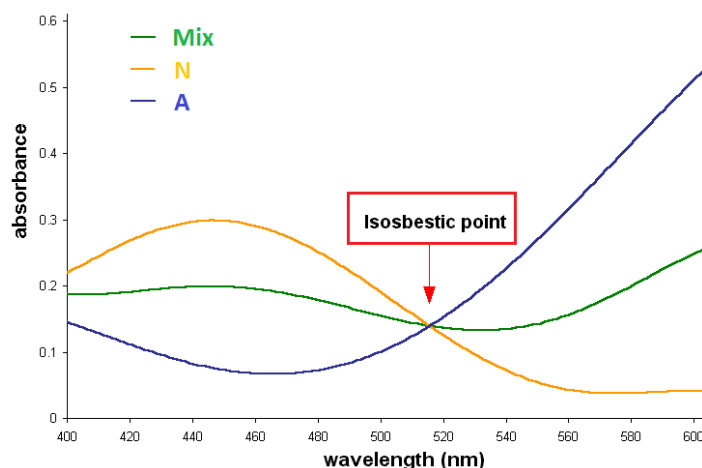


Figure 3: The spectra of basic (anion - A), neutral form (neutral - N), and a mix between both species (neutral and anion) are presented. All solutions have the same concentration of the analyte (10).

1.1.4 UV/VIS spectrophotometer

Spectrophotometers are instruments for measuring absorbance, reflectance or transmittance. The apparatus consists of a light source (lamp), monochromator (which allows a narrow source of light), sample container, the detector (that converts light energy into electrical signal) and the signal processor (which allows evaluation of the signal) (Figure 4) (1).

As a light source two lamps are routinely used. For the VIS range we use the tungsten lamp and for the UV range the deuterium lamp. The light source must produce sufficient power and stable radiation (6). To get monochromatic light from the continuous spectra a monochromator is used. It consists of the input slit, a mirror or lens, a prism or diffraction grating (which disperses polychromatic radiation), a focal lens, and the exit slit (11, 12). A sample container is a quartz cuvette, which is usually 1 cm long (11). The intensity of the transmitted light through the sample is measured by the detector, concretely by using a photomultiplier tube (1). Other types of detectors include a charge-coupled device (CCD), a photodiode or a photodiode array. Scanning monochromators, which serve as light filters, are used with single photodiode detectors and photomultiplier tubes. This light filtering ensures that the only light reaching the detector is the light of a single wavelength at one time. By using the scanning monochromator, the diffraction grating can be moved so it "steps-through" each wavelength and its intensity can be measured as a function of wavelength (1, 11).

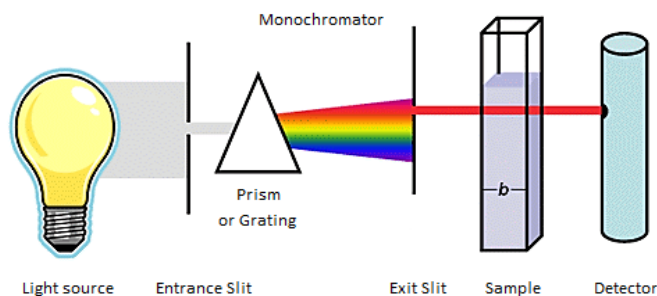


Figure 4: Scheme of UV/VIS spectrophotometer (13).

1.2 Fluorescence spectroscopy

The use of fluorescence in the biological and chemical sciences has increased remarkably in the past 20 years. Advances in technology have contributed to the performance of fluorescence spectroscopy and time-resolved fluorescence enabling the aforementioned methods to be executed without great difficulty. Fluorescence detection is highly sensitive, therefore relinquishing the need for extra expense and difficulties occurring during most biochemical measurements. For this reason, they have become primary research tools in biochemistry and biophysics. By using fluorescence techniques, intracellular molecules can be measured and localized even at single-molecule detection level. Fluorescence spectroscopy offers thorough analysis of fluorescence from a sample (14).

1.2.1 Phenomena of fluorescence

Substance in electronically excited-state emits light which is called luminescence. We divide it into phosphorescence and fluorescence, regarding the excited-state nature. Fluorescence emission rates are usually 10^8 s^{-1} , so typical fluorescence lifetime (τ) is near 10 ns (14). The phenomena of fluorescence appears when an orbital electron of an atom or a molecule, that has been excited by the absorption of electromagnetic radiation, relaxes back to its ground-state and by that emits a photon from an excited singlet-state. Typically the absorbed radiation has shorter wavelength and higher energy than the emitted light, which has a longer wavelength and lower energy. This can be described as the Stokes shift (Figure 5). Absorbed electromagnetic radiation can be intense, and in that case one electron may absorb even two photons. The two-photon absorption leads to emission of radiation with a shorter wavelength than the absorbed radiation. And finally, "resonance fluorescence" happens when the emitted radiation is of the same wavelength as the absorbed radiation. The glowing of fluorescent materials stops at the same moment when

the radiation source ends, which is not the same as phosphorescence where light emission continues to last for some time (14).

Excitation spectra is recorded during measurement of the emission intensity at constant wavelength (generally the emission maximum), and the wavelength of excitation varies. Vice versa, fluorescence spectra is recorded at constant excitation wavelength. The absorption and emission spectra for the same molecule are very similar (14).

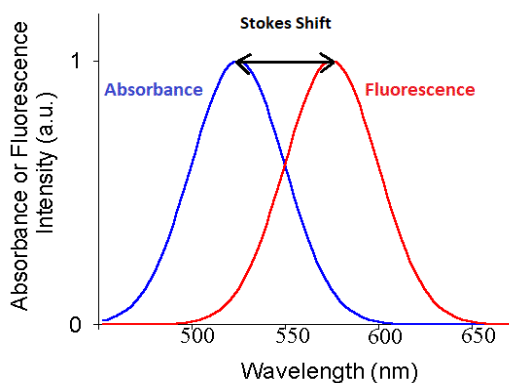


Figure 5: Stokes shift; the difference observed between both band maxima of the absorption and emission spectra of the same electronic transition.

1.2.2 Jablonski diagram

Jablonski diagram describes processes that appear between the absorption and emission of light (Figure 6). It represents a number of electronic energy levels of fluorophores (0, 1, 2, etc.). The singlet ground, first, and second electronic states are denoted by S_0 , S_1 , and S_2 , respectively. A fluorophore is a compound that absorbs the light of a specific wavelength and re-emits light at a longer wavelength (15).

Fluorophore is in the ground-state first and is excited by the light absorption to some higher vibrational level of either S_1 or S_2 . With some rare exceptions, the rapid relaxation of the molecules from S_2 to the lower vibrational level of S_1 occurs. This is described as internal conversion and is normally complete before the emission. Therefore, fluorescence emission comes from the lower energy vibrational level of S_1 . The vibrational energy levels of the excited-state have similar spacing to that of the ground-state. Because of this, visible vibrational structures in the absorption and the emission spectra have similarities. From the S_1 state, molecules can go to the first triplet state T_1 as well. This conversion is called intersystem crossing. Phosphorescence is the emission of light from T_1 and is shifted to longer wavelengths in comparison to the fluorescence (14–16).

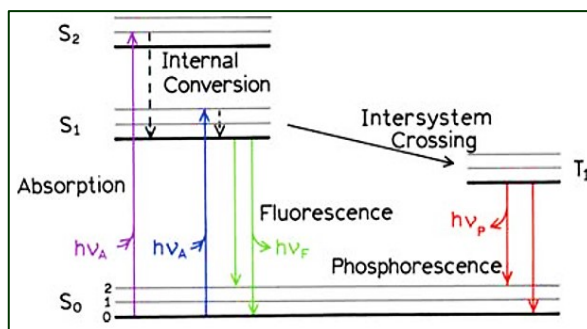


Figure 6: Jablonski diagram (14).

1.2.3 Fluorescent labelling

Fluorophores normally contain several combined condensed aromatic groups, or cyclic or planar molecules with many π bonds. Fluorophores can be divided into two main classes: intrinsic and extrinsic. Intrinsic fluorophores contain the part responsible for fluorescence present in their structure and they are the so-called »natural« fluorophores. Intrinsic fluorophores include the aromatic amino acids, flavins, NADH, derivatives of pyridoxyl and chlorophyll. Other extrinsic fluorophores are used for providing fluorescence in the sample when none exist after appliance, or for altering the spectral properties of the sample. Such substances include fluorescein, rhodamine, dansyl, and many other substances (Figure 7) (14, 15).

Normally proteins or other key biomolecules do not show an intrinsic fluorescence that can be used for a specific identification, characterization or for investigating different biomolecular processes. Fluorophores are bonded covalently to the biomolecules of interest. The result is fluorescent biomolecule conjugate, serving as a marker, which emits extrinsic fluorescence derived from tags that can be used to identify biomolecules (antibodies, peptides, nucleic acids) in a mixture with other biomolecules or in cells (15). Fluorescent markers are used to measure the concentrations of various anions and cations, reactive oxygen species (ROS), intracellular changes in pH and for the visualization of cell cultures (17).

Main important properties of fluorophores are:

- **Maximum excitation and emission wavelength [nm]:** similarity in the peaks of the excitation and emission spectra. Absorption and emission spectra should be both narrow (in order to reduce the possibility of interference due to overlapping spectra) (15).

- **Extinction coefficient** (or molar absorption, in $\text{mol}^{-1} \text{cm}^{-1}$): the quantity of absorbed light, at a given wavelength linked to the concentration of fluorophore in solution. Should be high enough to allow a selective and exclusive excitation.
- **Quantum yield**: how efficient is the energy transfer from incident light to emitted fluorescence (it is a number of emitted photons per absorbed photons). They must have high fluorescence quantum yield (for a sensitive detection in the presence of autofluorescence from the sample).
- **Lifetime**: the information about time, that a fluorophore spends in the excited-state before it emits a photon and returns to the ground-state. It can vary from picoseconds to hundreds of nanoseconds, depending on the fluorophore.
- **Stokes shift**: reduction in energy of the emitted photon compared to the absorbed photon. The shift should be observed between both band maxima of the absorption and emission spectra of the same electronic transition (8, 14, 18).

Other important parameters are: the polarity of the fluorophore molecule (it should be sufficiently soluble in physiological aqueous environments), the size and shape of the fluorophore, including the chemical structure, which allows tuning and controlling optical properties of the fluorophores. Last but not least, they must be highly photostable (having the ability to be re-excited as many times as possible before photochemically degrading) (15).

Acidity constant ($\text{p}K_{\text{a}}$) of fluorescent dyes plays an important role because it enables us to see how the dye will behave in both ground- and excited-state (assessment of the photoacidic properties of the fluorescent dyes according to the formation of the excited-state proton transfer reaction (ESPT)). The ESPT reaction is a fundamental and complex reaction that assists the design of new fluorescence markers. Moreover, it plays a major role in biological systems. It is responsible for the photostability of the DNA and for the behaviour of the green fluorescence protein. $\text{p}K_{\text{a}}$ is the equilibrium constant for a dissociation of the acid-base reactions. The greater the value of $\text{p}K_{\text{a}}$ or pH , the weaker the acid and the stronger the base. Knowledge of $\text{p}K_{\text{a}}$ values is necessary for the identification of cells that have proven themselves suitable for the fluorescent marker (labelling more acidic or basic cells) (19, 20).

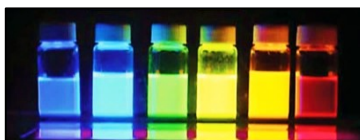
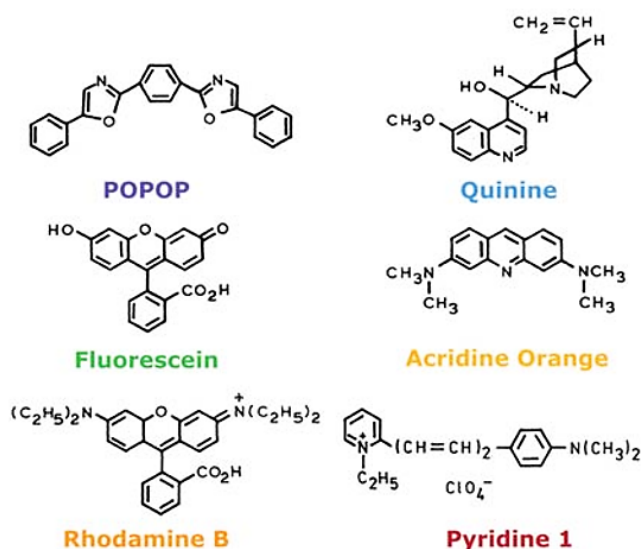


Figure 7: Structures of typical fluorescent substances (14).

1.2.3.1 Fluorescein

The well-known xanthene molecule fluorescein was first synthesized by Adolf von Baeyer in 1871. Fluorescein remains one of the most widely used fluorophores. It is used as a marker for many applications because of its good spectral characteristics: high molar absorptivity and excellent quantum yield. It is a versatile core dye that can be modified further to tune properties such as pK_a or excitation and/or emission wavelengths (21).

Fluorescein structure is constructed of two parts: the benzoic acid moiety (photocausated electron transfer donor) and the xanthene ring (fluorophore part of the molecule) (Figure 8). Considering its chemical structure, fluorescein appears in four different prototropic forms in aqueous solutions, which depend on the pH: cation, neutral, monoanion and dianion (Figure 9) (20).

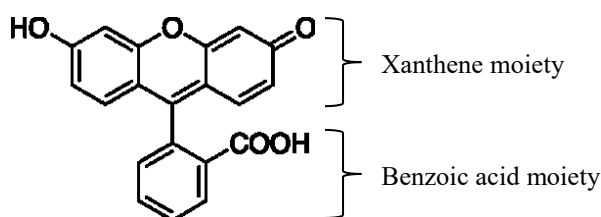


Figure 8: Fluorescein structure.

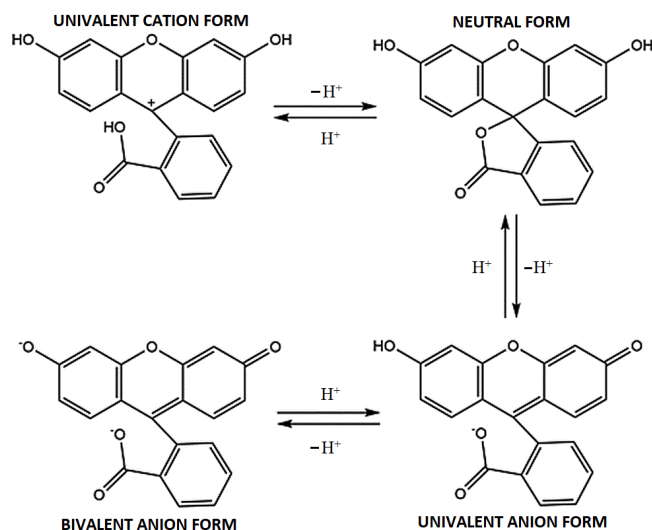


Figure 9: Four different prototropic forms of fluorescein: cation, neutral, monoanion and dianion (22).

Fluorescein is interesting when it comes to studying the excited-state. A fast pulse of light brings the fluorescein in the solution in excited-state and different excited prototropic forms of fluorescein are not in equilibrium anymore. This happens due to the preferential excitation of one or more of the fluorescein forms. Differences in the values of the equilibrium constants in the excited-state (pK_a^*) in comparison to the ground-state occur as well. Consequently, different excited forms of the fluorescein tend to interconvert through ESPT reactions and try to achieve equilibrium during their lifetimes. At low buffer concentrations the excited-state monoanion-dianion proton transfer reaction of fluorescein is too slow and because of that, it does not have a relevant effect on steady-state fluorescence intensity versus pH during the short lifetimes of these anions. However, if a suitable-proton donor acceptor is added, phosphate ions for example, monoanion-dianion proton transfer reaction in the excited-state appears very readily between the two observed species and the decays of both species become coupled. The ESPT reactions happening in xanthenic fluorophores have provided a distinct base for sensing the concentration of the elemental phosphate anion inside live cells in real time. Phosphate anions are important because they participate in signal transduction and energy storage in cells and extracellular media (20, 21, 23).

1.2.3.2 ESPT reaction

Use of specific fluorophores requires a complete understanding of the complexity of its photophysics. We are mostly interested in the excited-state dynamics of the molecular

forms, which exist at near physiological pH values. The proton transfer reactions can provide the exact knowledge in order to correctly interpret the experimental data obtained with the fluorophores that have different prototropic forms (24).

The occurrence of ESPT reactions is associated with light absorption, which often changes the electron distribution of a fluorophore, therefore causing changes in its physical or chemical properties. Because of the excited-state processes, time-dependent decays can be observed and characterized. The most prevailing type of an excited-state reaction is the loss or gain of protons (21, 24).

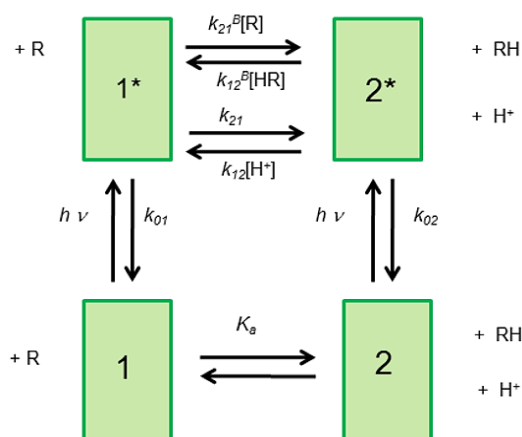


Figure 10: Kinetic scheme of a compartmental system for both states of the ESPT reaction, which is promoted by an appropriate proton donor/acceptor (20).

Species 1 and 2 are the molecules in the ground-state (Figure 10). Photoexcitation creates the excited-state species 1* and 2*, which can decay via fluorescence (F) and non-radiative (NR) processes (internal conversion and intersystem crossing). These processes are described by composite rate constants, depicted by $k_{01}(= k_{F1} + k_{NR1})$ and $k_{02}(= k_{F2} + k_{NR2})$. k_{12} and k_{21} represent the excited-state deprotonation and protonation rate constants, respectively. The buffer acid and base species are depicted by HR and R, respectively. They are suitable proton donors/acceptors for the buffer-mediated excited-state protonation (k_{21}^B) and deprotonation (k_{12}^B) (24). k_{21} represents unimolecular dissociation kinetic constant, while k_{12} represents the second order constant for the association. All these constants are positive. Acid and basic proton donor/acceptor forms, which are represented by RH and R do not affect 1 and 2 ground-state balance (20). Once the rate constants are known, the model equations may predict the fluorescence decay times as a function of the

pH and total buffer concentration, and the comparison of the predicted values to the experimental data can be made (24).

With the ESPT reaction we can determine pK_a and pK_a^* of our compound. Only when these values are within 6-8, the compound can be used to monitor phosphate ions inside cells in *in-vivo* tests. This is why the knowledge of the kinetic parameters, such as constants k_{21} and k_{12} is extremely important and necessary.

1.2.4 Spectrofluorometers

The basic components of a spectrofluorometer are similar to the components of an absorption spectrophotometer. The difference is that the fluorometer obtains two monochromators. The instrument consists of a xenon lamp as a high intensity exciting light source, monochromators for selecting both the excitation and emission wavelengths, versatile sample holder for a cuvette and the detector (Figure 11) (14, 25).

At the excitation wavelength of an analyte in a sample, the light source is employed. The light from the excitation monochromator passes through the sample and excites the analyte. After the excitation pulse, the relaxation of the analyte occurs by emitting the light at an emission wavelength longer than the excitation wavelength. The emitted light goes through the emission monochromator, which is in a suitable position due to the excitation light, and by that minimizes scattering of light and monitors it before it reaches the detector. The detector measures the emitted light, displays the fluorescence value and gives information about the fluorescence properties of the analyte. The output is usually presented graphically and stored digitally (14).

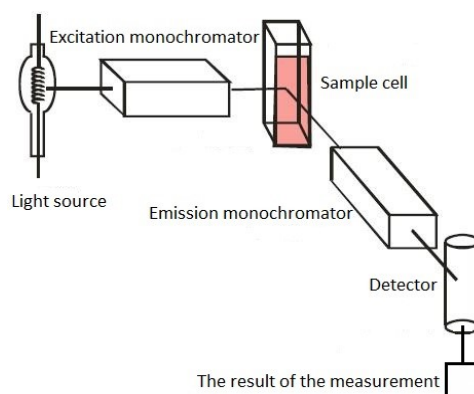


Figure 11: Schematic representation of a spectrofluorometer.

1.2.5 Time-resolved emission spectroscopy (TRES)

Time-resolved fluorescence spectroscopy is an extension of fluorescence spectroscopy. With this method, the fluorescence of a sample is screened as a function of time after the excitation pulse of light (decay associated spectra) (26).

The use of TRES can provide detailed information about the fluorescence features of our compound. The ESPT reaction mediated by phosphate should exhibit a double-exponential decay behavior, where decay times are independent of the wavelength of emission but dependent on the forward and reverse rates of the ESPT reaction. From the fluorescence spectra observed at distinct times during the fluorescence decay, detailed information about the ESPT reaction between the two prototropic forms of the specific fluorophore can be provided. Thus, as a result we obtain a 3-D surface that can be "sliced" to allow the temporal evolution of the fluorescence to be monitored and as well the resolution of spectrally overlapping species. It can be used to provide information of fluorophore mixtures and relaxation of the solvent. It is also possible to distinguish between scattered excitation light and impurity fluorescence (26, 27).

1.3 Fluorescence lifetime imaging microscopy (FLIM)

Fluorescence microscopy enables the observance of cellular activity in real time. It is an exceptional tool, by which a variety of cellular processes and interactions that are significant for understanding cell physiology can be explained. Sensing certain analytes intracellularly is crucially important to understand the relationship between cellular pH and metabolic states or the roles of specific ions in signaling pathways (17).

The use of fluorescence lifetimes for quantitative determination is a strong alternative to ratiometric, intensity-based fluorescence microscopy methods. The molecules that have been excited by a pulse of light show an exponential decay kinetics, with a lifetime of fluorescence typically in the order of a few nanoseconds. Experimentally, we measure the fluorescence lifetime in the frequency domain or in the time domain by using the methodology of single-photon timing (SPT). The SPT method uses all photons that reach the detectors, raster scans the sample and collects a single fluorescence decay trace in each pixel of the image (Figure 12). The excitation laser is set in a confocal mode and focused on the sample, the pulsed laser is aimed towards the specimen, and with the help of point detectors collected fluorescence is detected (28).

Specific hardware is used in order to correlate the arrival time of each individual photon in SPT mode. The FLIM technique is multidimensional because the FLIM image consist of both intensity (total number of photons) and lifetime information. At FLIM the fluorophore's lifetime does not depend on its concentration or the power of the excitation source, which is its primary advantage. It also permits time gates to be set to distinguish between photons arriving at different times after the light excitation. This potential helps especially when it comes to discriminating between photons, that are emitted via cell autofluorescence and those emitted by fluorescent dyes, having a different, longer lifetime. The aforementioned serves as a filter to exclusively obtain the signal from the fluorescence marker and avoid other interference from the cell (17, 20, 28, 29).

By using the FLIM method, the behavior of our compound in the media, that mimics the cellular interior, and also specifically in cultivated cells can be observed. Images, that serve as a tool for studying the lifetime of the fluorescence of the compound can be obtained. This method allows the detection of important analytes, such as phosphate ions which are the analyte of choice in our case. It can be determined whether the compound is suitable as a cell marker.

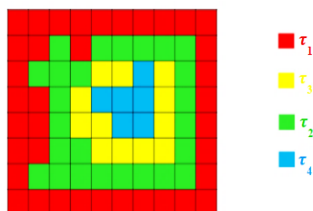


Figure 12: FLIM image example. Fluorescence lifetimes are codified by colours, producing an image (20).

2 RESEARCH AIM AND OBJECTIVES

Dyes with near-red emission are certainly interesting in the field of cell biology because of their undoubted benefits - excellent photophysical characteristics. For employment of such dyes it is necessary to have in-depth understanding of their photophysics.

Within the framework of this Master's thesis we will explore photophysical behavior of the new silyl-xanthene derivative, **2-Me-4OMe-TM**:

- The absorption and emission spectra of prototropic forms of aqueous solution of our derivative will be examined at steady-state, within the range of different pH values.
- pK_a will be calculated in both steady- and excited-state, by using absorption spectroscopy and by applying the thermodynamic theory all the while considering Beer-Lambert law and adjusting the experimental data using nonlinear least square regression.
- We will observe whether the ESPT reaction will take place between the neutral and the anion species of our compound in aqueous solutions at near-neutral pH (mediated by the presence of an adequate concentration of phosphate buffer), by using emission spectroscopy in steady-state and time-resolved spectroscopy.
- Due to the existence of this reaction, we will obtain decay-time emission spectra (in the time range of nanoseconds - TRES).
- The effect of different concentrations of phosphate buffer on the dye decay times of the fluorescence will be studied by emission spectroscopy with temporal resolution in solution and by FLIM in media that mimics the cell interior.
- If the results from the previous studies prove to be satisfactory (depending on whether the ESPT reaction is formed), HEK 293 cells will be grown during the cell differentiation phase and then loaded with the dye in order to detect penetration of the phosphate into the cell interior.
- Finally, by using FLIM we will determine whether our derivative could be used as a real-time phosphate intracellular marker in cultured cells.

3 MATERIALS AND METHODS

3.1 Materials

3.1.1 Reagents

a) Preparation of solutions:

- phosphate buffer solutions: sodium phosphate dibasic dihydrate ($\text{Na}_2\text{HPO}_4 \times 2\text{H}_2\text{O}$, $M=177,99$ g/mol) and sodium phosphate monobasic dihydrate ($\text{NaH}_2\text{PO}_4 \times 2\text{H}_2\text{O}$, $M=156,01$ g/mol), both Sigma-Aldrich (Germany)
- sodium hydroxide pellets (NaOH , $M=40,00$ g/mol), Panreac (Spain)
- Trizma® base ($\text{C}_4\text{H}_{11}\text{NO}_3$, $M=121,14$ g/mol), Sigma-Aldrich (USA)
- Dulbecco's Modified Eagle Medium (DMEM, D-6546), Sigma Chemical (St. Louis, MO)
- potassium chloride GR for analysis (KCl , $M=74,56$ g/mol), Merck (Germany)
- perchloric acid 70 % (HClO_4 , $M=100,46$ g/mol), Sigma-Aldrich (Germany)
- commercially available phosphate-buffered saline (PBS), Sigma-Aldrich (Germany)

b) Solvents:

- Milli-Q water (ultrapure water of Type 1 - bidistilled, deionized water)
- ethanol absolute GR for analysis ($\text{C}_2\text{H}_5\text{OH}$, $M=46,07$ g/mol), Merck (Germany)
- NaOH (different molarities, already prepared - diluted before use, if necessary)

The fluorescent dye 2-Me-4OMe-TM (Figure 13) was synthesized by the group of Juan Manuel Cuerva Carvajal (organometallic chemistry and molecular electronics), from the Department of Organic Chemistry at the Faculty of Science of the University of Granada, Spain (30–32).

Chemical name: 7-hydroxy-10-(4-methylphenyl)-5,5-dimethyldibenzo[b,e]silin-3(5H)-one

Chemical formula:

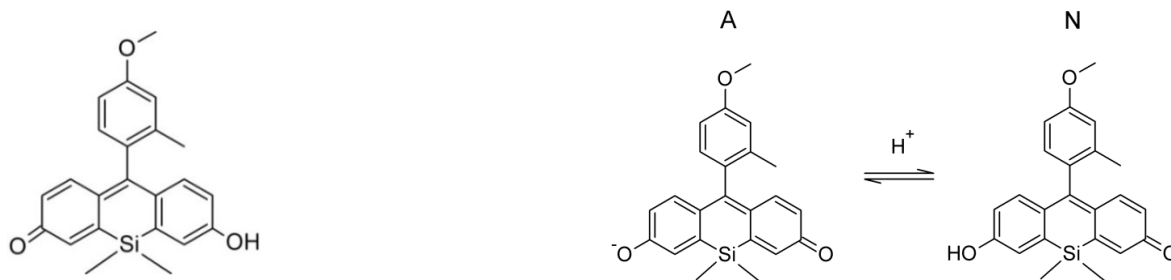


Figure 13: Fluorescent dye **2-Me-4OMe-TM** and its two prototropic forms (A - anion, N - neutral, respectively).

Molecular weight: 374.5 g/mol

3.1.2 Laboratory equipment

- **Micropipettes (single channel)**

1 - 5 ml (Biohit, Germany)

100 - 1000 μ l (Gilson, France)

20 - 200 μ l (Thermo Scientific, USA)

5 - 50 μ l (BOECO, Germany)

0,5 - 10 μ l (BOECO, Germany)

With appropriate accessory tips

- **Laboratory glassware and other research equipment**

volumetric flasks with stoppers (10 ml, 25 ml, 50 ml, 100 ml)

beaker (10 ml, 50 ml, 100 ml, 500 ml, 1000 ml)

glass Pasteur pipettes with rubber dropper

plastic Pasteur pipettes

quartz cuvettes

plastic tubes with plastic stoppers (5 ml, 12 ml)

plastic centrifuge test tube vial container, self standing with a cap (50 ml)

filters (wideness of pores 0,02 μ m)

injection syringes

tube rack

stainless laboratory spatula

3.1.3 Instrumentation

- Sartorius analytical balance instrument A-120S (Germany)
- PerkinElmer Lambda 650 UV/VIS spectrophotometer with temperature controller (Waltham, Massachusetts)
- JASCO FP-6500 spectrofluorometer with temperature controller (Japan)
- FluoTime 200 fluorometer (PicoQuant GmbH, Germany)
- MicroTime 200 fluorescence lifetime microscope system (PicoQuant GmbH, Germany)
- pulsed lasers LDH-440, LDH-470, LDH-530 (PicoQuant, Germany)
- pH-meter Crison (model GLP-22, Spain)
- ultrasonic bath ULTRASONICS (P SELECTA, Spain)
- apparatus for water purification MERCKMILLIPORE (USA)
- refrigerator (3°C)

3.2 Methods

For our research we selected, as previously mentioned, the xanthene based fluorescence dye **2-Me-4-OMe-TM**. The compound shows pH dependency. The pure compound is in solid aggregate state, stored in a glass vial (in the form of a red powder).

2-Me-4-OMe-TM was added right before the recording of each spectra. By means of a pH meter, calibrated with Crison standard tampons, the pH values of the prepared solutions were measured following the manufacturer's instructions. As to adjust the pH of the unbuffered aqueous solutions, NaOH 0.01 M and HClO₄ 0.01 M grade were employed. All the solutions were freshly prepared, if not immediately used, they were stored into a refrigerator. The chemicals were used as received.

The entire research work plan:

1. preparation of stock dye solution
2. preparation of aqueous solutions and phosphate buffers
3. preparation of solutions for the measurements
4. measuring absorbance with UV-VIS spectrophotometer
5. measuring fluorescence with a fluorescence spectrophotometer
6. measuring pH of the solutions immediately after recording each spectra
7. measuring fluorescence decay traces with fluorometer

8. performing confocal fluorescence microscopy
9. evaluation of the measurements

3.2.1 Preparation of stock dye solution

2-Me-4-OMe-TM was dissolved in the required volume of purified water, 0.02 M NaOH and ethanol absolute. The dye was weighed (0.4 mg) into a small glass vial. The solvents were added as needed for complete dye dissolution. The volume needed to accomplish complete dissolution of the dye was 13.45 ml (H₂O = 7.2 ml, NaOH (0.02 M) = 1.65 ml, EtOH = 4.6 ml). The concentration of the stock dye solution was calculated according to equation 4, and was 7.94×10^{-5} mol/l. Moles (1.07×10^{-6} mol) were calculated with the application of equation 5:

Equation 4

$$C = \frac{n}{V}$$

Equation 5

$$n = \frac{m}{M}$$

C = concentration of the stock dye solution in mol per litre

V = volume of solvent needed to dissolve all the dye in litres

n = number of moles

m = mass of solute that we weighed in grams

M = molar mass of our compound in grams per mol

The stock dye solution was stored in a refrigerator as to remain protected from light exposure. From this stock solution, the required concentrations of **2-Me-4-OMe-TM** at the suitable pH and phosphate concentrations were prepared.

3.2.2 Preparation of phosphate buffer solutions

Several parallels of phosphate buffer solutions with different molar concentrations were prepared. Firstly, for the required concentration of the buffer, the mass of the NaH₂PO₄ and Na₂HPO₄ was calculated, weighed and then filled up with Milli-Q water, up to the top

mark on the volumetric flask. Calculation of the mass was performed (each time the certain concentration of the buffer was needed) according to the following equation 6:

Equation 6

$$m = C \times M \times V$$

m = mass of the weighed substance in grams

C = concentration in moles per litre

M = molar mass of each substance in grams per mol

V = volume of prepared solution in litres

3.2.3 Preparation of solutions for the measurements

3.2.3.1 Solutions for the pK_a calculation

A series of solutions of **2-Me-4-OMe-TM** (7.94×10^{-6} mol/l or 7.94×10^{-7} M, respectively) in 0.05 M and 0.005 M phosphate buffer with pH values in the range of 4.00 to 9.50 were prepared.

Solution concentrations were calculated following the equation 7:

Equation 7

$$C_s = \frac{C \times V_d}{V_{tot}}$$

C_s = concentration of the solutions in mol per litre

C = concentration of the stock dye solution in mol per litre

V_d = volume of pipetted stock dye solution into each solution in microlitres

V_{tot} = total volume of our solution in microlitres

3.2.3.2 Solutions for the TRES experiments

For the TRES experiments, a series of solutions of **2-Me-4OMe-TM** with the concentration of 7.94×10^{-7} mol/l in 0.7 M phosphate buffer with pH values in the range of 5.50 to 8.95 were prepared, and each solution was excited at 530 nm as to preferentially

excite the anion form. The decay traces were collected in the emission wavelength range from 550 to 650 nm.

3.2.3.3 Solutions for the FLIM experiments - in DMEM

2-Me-4OMe-TM was dissolved in solutions of DMEM and 20 mM TRIS buffer, at pH 7.35 (near physiological pH) and different phosphate concentrations in the 0 to 300 mM range were employed. Milli-Q water was used as a solvent for the preparation of all solutions. The dye was at the concentration of 1×10^{-7} M. The solutions were stored in a cool and dark place when not in use as to avoid possible degradation by light and heat.

3.2.3.4 Solutions for the FLIM experiments - the HEK 293 cells

The HEK 293 cells were provided by the Cell Culture Facility, University of Granada, Spain. The HEK 293 cells were grown in DMEM containing 10% foetal bovine serum (FBS) and 1% penicillin-streptomycin in a humidified 5% incubator with CO₂. To carry out the FLIM microscopy experiments, the cells were planted onto 25 mm coverslips in six-well plates at a density of 11250 cells*cm⁻². Before the measurements, we washed the cells twice with commercially available phosphate-buffered saline (PBS), pH 7.35. The working solutions were prepared using PBS medium and **2-Me-4OMe-TM** at the concentration of 4×10^{-7} M.

3.2.4 Measuring the absorbance with the UV-VIS spectrophotometer

A Perkin-Elmer Lambda 650 UV/VIS spectrophotometer with a temperature-controlled cell and 0.17 nm UV/VIS resolution was employed as to record the absorption spectra. It is a dual sampling compartment spectrophotometer which is compatible with transmission and reflectance measurements. The wavelength range amounts from 190 to 900 nm. The large sample compartment carries an automated polarizer/depolarizer drive that provides or allows further depolarization of oriented samples with polarized light. It is equipped with a beam depolarizer that corrects instruments' bias. It has a deuterium and tungsten halogen light source which is prealigned and prefocused for quick replacement and maximum uptime as well as double holographic grating monochromators for ultra-low stray light performance. The system and all the components that are part of it are controlled by a computer with suitable software (20).

Protocol:

- Before we began with the experiment, we turned on the instrument and entered the program by using the appropriate password.
- When entering the program, firstly, we needed to set the measurement range in which we measured our sample solutions. We selected the wavelength interval from 400 to 650 nm.
- We took two cuvettes and washed them several times with purified water, then we filled them with purified water and later inserted them into the device to measure a »blank« sample first (for the baseline).
- Next, we continued with sample measurements. We took the cuvette, which had been previously used to determine the baseline, and washed it with a small amount of the sample solution, poured out the residue and then filled it again. The filled cuvette was inserted into the device to start the measurement.
- In between each measurement, we washed the cuvette several times with purified water and then again using a small amount of each following sample.

3.2.5 Measuring the fluorescence with a fluorescence spectrophotometer

Emission spectra were recorded on JASCO FP-6500 spectrofluorometer with a temperature controller. It uses a DC-powered 150 W xenon lamp as a source (in a sealed housing) with a photometric rationing system. The detector is a silicon photodiode for excitation and a photomultiplier for emission with a wavelength covering from 200 to 900 nm. The FP-6500 provides extremely high sensitivity with a signal to noise ratio greater than 200:1 Raman band of water peak-to-peak, using spectral bandwidths 5 nm on both excitation and emission monochromators, 2 s response time at 350 nm excitation wavelength. It has single position water thermostatable cell holder. Spectral bandpass can be selected from 20 to 1 nm for when high resolution is required. Wavelength scan speed is also a controllable parameter, within the speed from 10 to 20000 nm/min depending on the selected response and sensitivity (20).

Protocol:

- First, we turned on the computer.
- Next, we turned on the fluorescence spectrophotometer, which needed some time to become ready for use.

- We entered the program Spectra Manager, then set the measurement on emission and defined a method at which we will obtain the optimal ratio between the signal to noise.
- We created a folder for data storage.
- We took a completely clean cuvette with 4 transparent sides, washed it with a small amount of the sample and filled it with an actual sample.
- The outer surface of the cuvette was wiped dry using an appropriate paper towel (all 4 sides in order to avoid impurity and not to disturb the measurements).
- We measured the fluorescence for each sample solution.

3.2.6 Measuring with time-resolved fluorometer

Time-resolved fluorescence measurements were performed in a FluoTime 200 instrument (PicoQuant GmbH), based on time-correlated single photon counting (TCSPC) and provided with an excitation pulsed laser. This device has a high performance fluorescence lifetime system including single photon timing sensitivity, modular construction and research flexibility. It is equipped with the complete electronics and optics for recording fluorescence decays with TCSPC. The system is used with picosecond diode lasers and optimized for high temporal resolution. With the FluoTime 200, decay times down to a few picoseconds can be resolved. The system permits operating at laser repetition rates as high as 100 MHz and count rates up to several million counts per second (20, 25).

TCSPC unit measures the time between excitation and fluorescence emission. In TCSPC, the laser pulse or a photodiode provides a required defined “start”, and a defined “stop” signal, realized by detection with single-photon sensitive detectors. The measurement is repeated many times as to account for the statistical nature of the fluorophores emission. The delay times are then sorted into a histogram which portrays the occurrence of emission over time after the excitation pulse (20, 26). TCSPC data acquisition unit is available - TimeHarp 200. Measurement data were in our case transferred to the FluoFit software (PicoQuant Inc.) directly for global decay analysis (20, 26).

Protocol:

- First we chose the appropriate laser, connected it properly and turned on the device by turning the key in the front of the device.
- We set the intensity of the laser.
- We entered the software and set the desired emission wavelength.

- First we measured dispersant (LUDOX as scatter) to determine instrument response function (IRF).
- Then we measured sample decays which needed to reach 2×10^4 counts on the peak channel. The calibration of the instrument needed to be executed prior to the measurements.

3.2.7 Measuring with inverse time-resolved confocal fluorescence microscope

The system used to perform FLIM measurements is based on a confocal microscope with pulsed laser excitation (MicroTime 200, PicoQuant GmbH), capable of fluorescence life-time measurements, FLIM, Fluorescence Correlation Spectroscopy (FCS) and single-molecule sensitivity detection. It is equipped with SymPhoTime 64 software (28).

MicroTime 200 consists of 4 parts:

- **Olympus IX71 inverted microscope** (Figure 14).

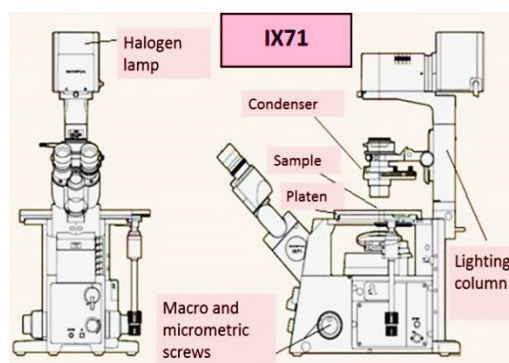


Figure 14: Olympus IX71 inverted microscope scheme (33).

- **Excitation system** (picosecond diode lasers).
- **Main Optical Unit (MOU)**, which contains subunits (Figure 15):
 - The excitation segment: where the laser light beam comes from.
 - Basic confocal unit: separating fluorescence signal from the excitation light.
 - Focal plane diagnosis: CCD camera allows the diagnosis and it permanently monitors the image seen by the lens. The obtained images are displayed on the computer.
 - Detection channels: fluorescent emission collimated beam reaches the detectors through the basic confocal unit. 50/50 radiation separator separates the

fluorescence emission into two equivalent detection channels. The detectors used are individual photon avalanche diodes (SPAD) SPCM-AQR-14 (PerkinElmer).

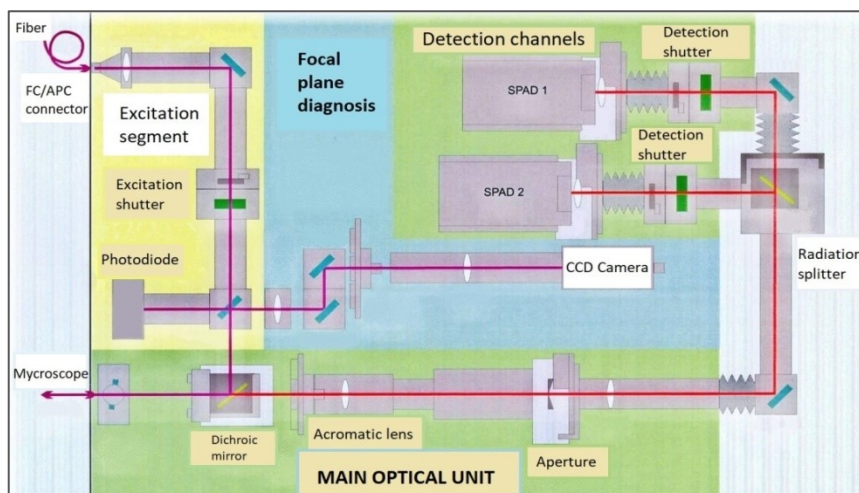


Figure 15: MOU scheme (20).

- **Data acquisition and electronic control:** 2 TimeHarp 200 data collection targets (each one for each detection channel). It is a TCSPC system that can operate in several ways, the most important is time-tagged-time-resolved (TTTR). The TTTR methodology is performed for the analysis of individual molecules (20).

Protocol:

- First we chose the appropriate laser, connected it properly and turned on the device.
- We entered the software and set the desired excitation and emission wavelength.
- The calibration of the instrument needed to be executed prior to the measurements.
- We prepared the microscope system Olympus IX71 (set the oil immersion onto the objective).
- Prepared solutions were plated onto the surface of a microscope glass slide, and confocal images were recorded by performing FLIM.
- Data were collected by a TimeHarp 200 TCSPC module.
- Raw fluorescence intensity images were exported as matrix data by SymPhoTime 64 software and analysed by Fiji program (ImageJ) (34).

3.3 Evaluation of the measurements

Treatment of the results, their representation and nonlinear least squares analysis, were performed using the software program **OriginPro 8.5** (Northampton, Massachusetts,

USA). The equations from 9 to 16 were used for the processing of raw data obtained after measurements with the individual apparatus and served as supporting information. Equations were applied to the OriginPro 8.5 program so that we could obtain images of spectra, normalized spectra and other graphs that are displayed in the results section of the Master's thesis.

Reconvolution analysis and individual and global multiexponential adjustments were performed with the **FluoFit** software. This program uses an iterative reconvolution analysis, based on the equation 8:

Equation 8

$$F(t) = \int_0^t I(t-t')D(t')dt'$$

Where $F(t)$ is the experimental decay, $I(t)$ is the assumed decay function or impulse response function that represents the decay when the sample is excited with an infinitely short pulse, and $D(t')$ is the instrumental profile of the lamp. As an adjustment method, nonlinear least squares analysis was used through the Marquardt algorithm.

System software **SymPhoTime 64** was employed for the analysis of the FLIM measurements. Raw fluorescence intensity images were exported by SymPhoTime 64 software and analysed by **Fiji** program, where the images were also fitted.

3.3.1 Analysis of the experimental absorbance versus pH used to determine the ground-state equilibrium of 2-Me-4OMe-TM

If a neutral/anion system agrees with the Beer-Lambert law, at any wavelength (λ_{abs}) and pH, the absorbance (A) is given by the expression:

Equation 9

$$A(pH, \lambda_{abs}) = C \left(\sum_i \alpha_i(pH, pK_a) \varepsilon_i(\lambda_{abs}) \right) d$$

C is the total concentration of the **2-Me-4OMe-TM**, d stands for the optical path length, ε_i denotes the wavelength-dependent molar absorption coefficient of the i th prototropic form of **2-Me-4OMe-TM**, and $\alpha_i(pH, pK_a)$ is the fraction of **2-Me-4OMe-TM** in the i th

prototropic form, depending on both pH and pK_a (constant of the acid-base equilibria between the neutral and anion form of the dye in steady-state) (35).

Equation 10

$$\alpha_N = \frac{[H^+]}{H^+ + K_a}$$

Equation 11

$$\alpha_A = \frac{[K_a]}{H^+ + K_a}$$

3.3.2 Analysis of the experimental fluorescence versus pH used to determine the ground-state equilibrium of 2-Me-4OMe-TM

The total fluorescence signal $F(\lambda_{ex}, \lambda_{em}, [H^+])$ at proton concentration $[H^+]$ due to excitation at λ_{ex} and observed at emission wavelength λ_{em} can be expressed as:

Equation 12

$$F(\lambda_{ex}, \lambda_{em}, [H^+]) = \frac{F_{min}[H^+] + F_{max}K_a}{K_a + [H^+]}$$

F_{min} indicates the fluorescence signal of the neutral form of the dye and F_{max} denotes the fluorescence signal of the anion form of 2-Me-4OMe-TM. Fitting eq. 12 to the fluorescence data $F(\lambda_{ex}, \lambda_{em}, [H^+])$ as a function of $[H^+]$ yields values for K_a , F_{min} , and F_{max} (35).

3.3.3 Evaluation of kinetic parameters from the lifetimes at high phosphate buffer concentrations

If we excite the dye as shown in Figure 13 by an infinitely short light pulse, which does not significantly affect the concentrations of the ground-state species, then the fluorescence δ -response function, $f(\lambda_{em}, \lambda_{ex}, t)$, at emission wavelength λ_{em} due to excitation at λ_{ex} is given by:

Equation 13

$$f(\lambda_{em}, \lambda_{ex}, t) = p_1 e^{\gamma_1 t} + p_2 e^{\gamma_2 t}$$

$$t \geq 0$$

Eq. 13 has been written in the common biexponential format, where:

Equation 14

$$\gamma_{1,2} = \frac{-(a+c) \mp \sqrt{(c-a)^2 + 4bd}}{2};$$

$$a = k_{01} + k_{21} + k_{21}^B[R]; b = k_{12}[H^+] + k_{12}^B[RH]; c = k_{02} + k_{12}[H^+] + k_{12}^B[RH]; d = k_{21} + k_{21}^B[R].$$

$[R]$ and $[RH]$ are related to the total buffer concentration, $C^B = [R] + [RH]$, by the expressions $[RH] = C^B[H^+]/([H^+] + K_a^B)$ and $[R] = C^B K_a^B/([H^+] + K_a^B)$, where K_a^B is the dissociation constant for the reversible reaction $RH \leftrightarrow R + H^+$ (35).

The γ factors are related to the lifetimes τ_1 and τ_2 by the expression:

Equation 15

$$\tau_{1,2} = -\frac{1}{\gamma_{1,2}}$$

The rate constants k_{21}^B and k_{12}^B , along with the known value of K_a^B , can provide the excited-state pK_a^* according to the equation:

Equation 16

$$pK_a^* = \log(k_{12}^B) - \log(k_{21}^B) + pK_a^B$$

4 RESULTS AND DISCUSSION

4.1 General findings

Recently, silyl-substituted xanthene dye, named **2-Me-4OMe Tokyo Magenta (2-Me-4OMe-TM)** was synthesized. The oxygen atom at the 10-position of the xanthene ring has been replaced by a Si atom. This compound has been developed as a novel fluorescent dye, that maintains the key advantages of the parent structures, which are the narrow absorption and emission spectra, high extinction coefficient, high quantum yield, satisfactory lifetime and Stokes shift. The absorption and emission wavelengths of **2-Me-4OMe-TM** are both about 90 nm higher than the wavelengths of the fluorescein, with the emission being located in the near-red region, and fluorescing in red color.

During the preparation procedure our compound showed sensitivity to light. Therefore it was important to add dye to the samples just before each measurement. For future research and the use of our compound as a fluorophore, it would be wise to consider how to improve its photo-stability.

We came to the conclusion that the fluorescence of our compound is tied to the pH values. The structure of the compound alters due to the presence of H⁺ ions in a more acidic environment. Balance is then established between the neutral and anion form and molecules are fluorescing. At a basic pH it can be clearly seen, that the compound passes from neutral to ionized anionic form; it is well absorbed and fluoresced in the visible region. While at low pH values the fluorescence of the compound is barely visible.

4.2 Absorption measurements and ground-state equilibria

UV-VIS spectra of 10 aqueous solutions of **2-Me-4-OMe-TM** in the pH range between 4.92 to 9.13 and the concentration of 7.94×10^{-6} M, prepared with phosphate buffer at a concentration of 0.05 M, are shown in Figure 16. Our sample solutions were well absorbed in the visible range as can be observed from the spectra. The dependence of the fluorescent compound to the pH value is presented by the absorption spectra. The position of the absorption spectra maximum ($\lambda_{\text{max abs}}$) was the same at all pH values and at all the concentrations, suggesting no change when altering pH. Two spectroscopically distinguishable species were observed, which were converted into each other as the pH varied, and gave rise to the formation of one marked isosbestic point around the

wavelength of 524 nm ($\lambda_{\text{isosb point}}$). The appearance of the isosbestic point showed us that the absorbance of the compound at all pH values at $\lambda_{\text{isosb point}}$ is equal.

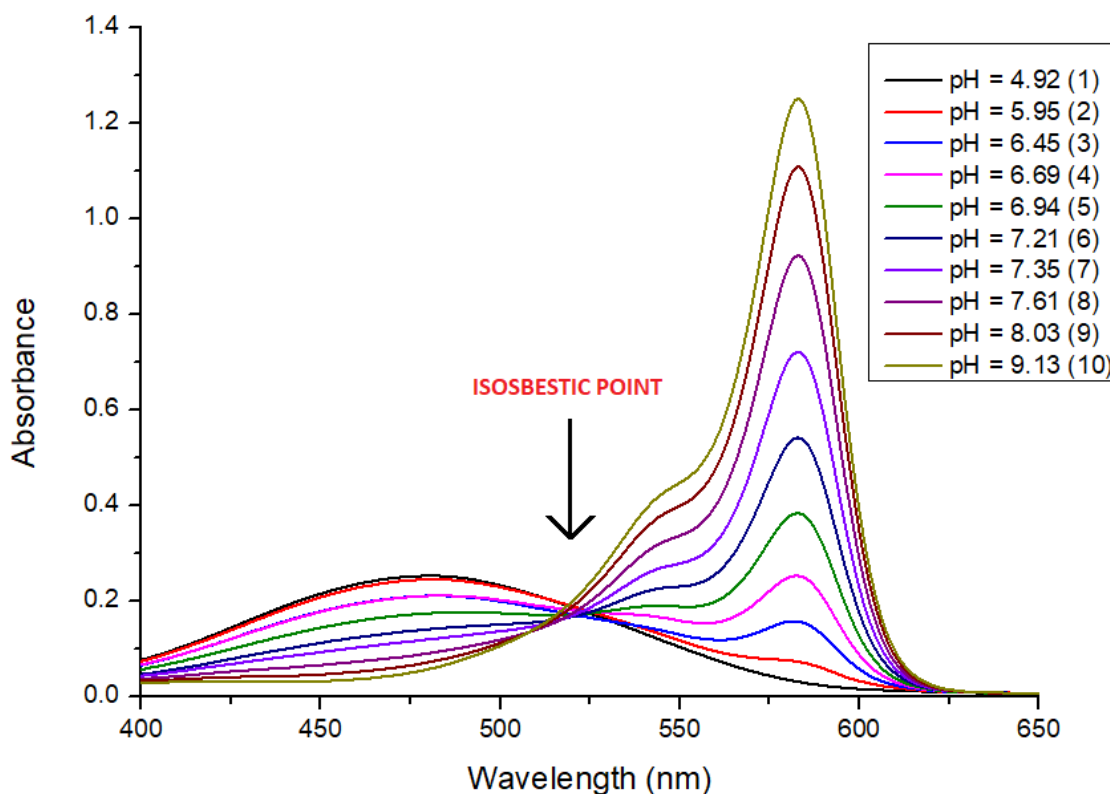


Figure 16: Absorption spectra of 7.94×10^{-6} M aqueous solutions of **2-Me-4OMe-TM** in the pH range between 4.92 to 9.13.

We suggest that the two prototropic species which absorb in the visible region of the spectra correspond to neutral and anionic form of the compound (Figure 17). The spectra of the solution at pH 9.13 (basic pH) was assigned to the anion with maximum absorbance peak located at 583 nm and a shoulder arisen at 550 nm (Figure 18). At a pH below 6.45, broad spectra with a diffuse maximum around 480 nm was observed which was assigned to the neutral species (Figure 18). The anionic form expressed greater absorbance than the neutral form. With decreasing pH, the shoulder disappeared and the band that peaks at 583 nm was blue-shifted, exhibiting a very broad profile.

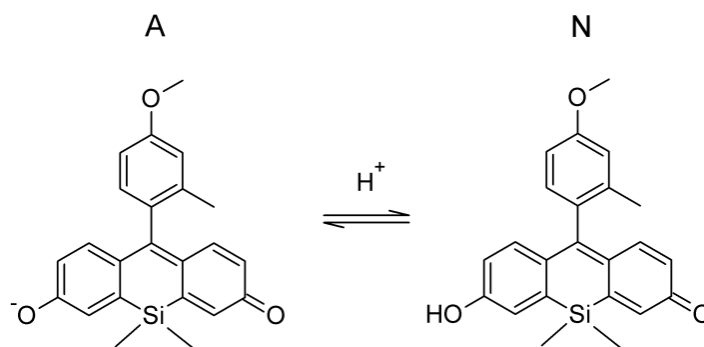


Figure 17: Prototropic forms of **2-Me-4OMe-TM**: A (anion), N (neutral).

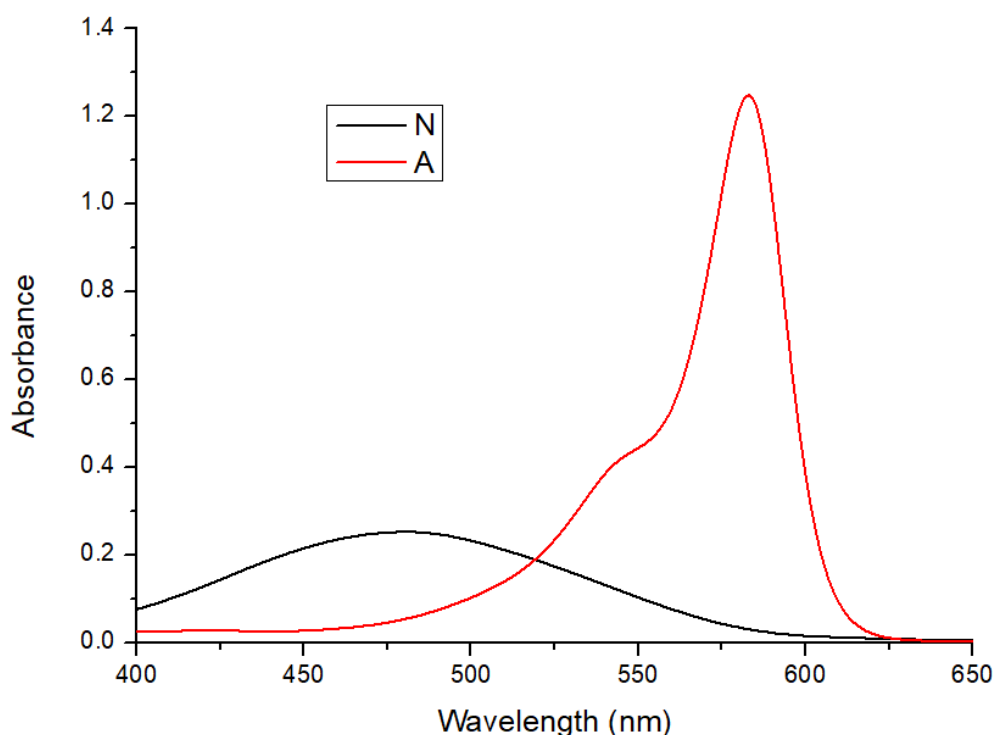


Figure 18: Absorption spectra for the **neutral** (black) and **anionic** (red) form of 7.94×10^{-6} M aqueous solutions of **2-Me-4OMe-TM**.

pH-induced transitions of **2-Me-4OMe-TM** due to ground-state proton-transfer reactions, dictated by the ground-state pK_a values, were observed. The only pK_a of interest for biological applications is the one that offers a near-neutral pH when combined with the dye (optimal pH results around 6.7 to 7.4, which are equal to the cytosolic pH of most cells). Thus, the dye with pK_a value around 7 is better retained in cells, which is a really important feature of fluorophores meant to stain live cells. Therefore, the value of pK_a of our compound was also of interest precisely because the compound could be used as a cellular marker. We performed the nonlinear global fitting of the complete surface of A vs. pH and

λ_{abs} to Beer's law and the equations of the acid-base equilibria (equations 9, 10, 11) allowed to determine the molar absorption coefficients $\varepsilon_i(\lambda_{\text{abs}})$, which are needed to obtain $\text{p}K_{\text{a}}$. In the fitting, the $\text{p}K_{\text{a}}$ was linked over the whole surface, whereas $\varepsilon_i(\lambda_{\text{abs}})$ was a locally adjustable parameter at each wavelength for each species. The absorbance data surface was composed of 10 pH values and 250 λ_{abs} values between 400 and 650 nm at each pH. The recovered parameters were independent of the values initially assigned to these parameters used for the fitting process. Figure 19 shows the estimated values of the molar absorption coefficients of the neutral (ε_{N}) and anionic forms (ε_{A}) of the dye at low phosphate buffer concentration (0.05 M). The recovered $\text{p}K_{\text{a}}$ value was 7.3 and is higher than that of fluorescein (~ 6.4), which is favorable and consistent with the previously stated. This value imposes on possible good behavior of our compound in the cells and its potential use as a fluorophore marker.

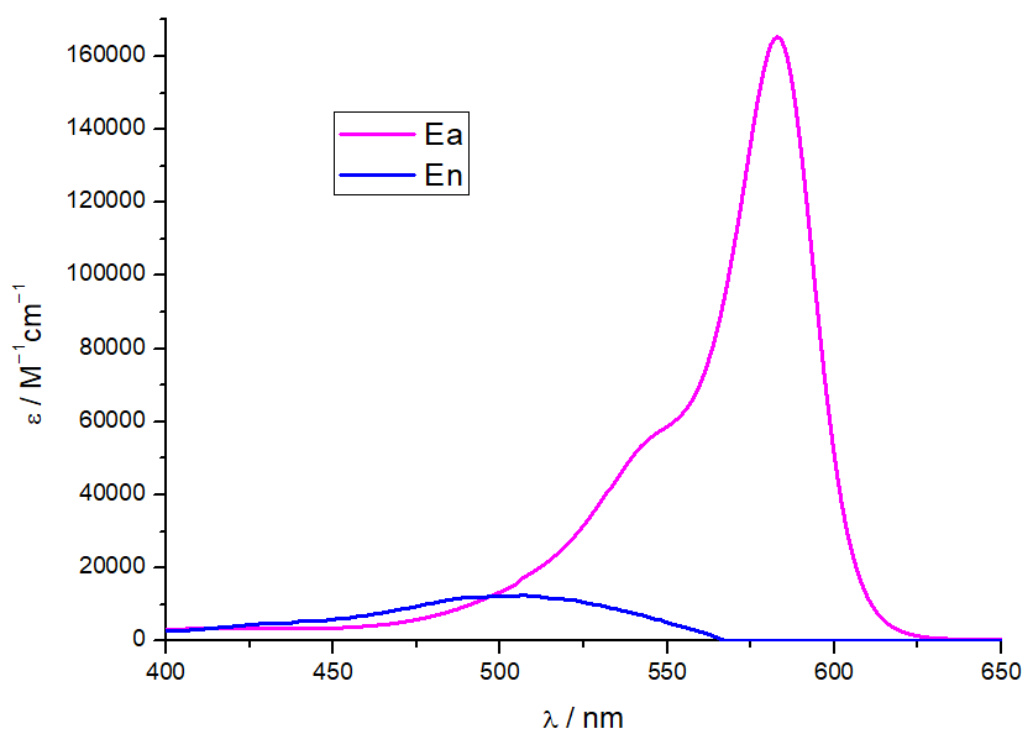


Figure 19: Recovered molar absorption coefficients versus wavelength for the **neutral** (blue) and **anionic** (pink) form of **2-Me-4OMe-TM**.

4.3 Steady-state emission spectra

Steady-state emission spectra of **2-Me-4OMe-TM** at the concentration of 7.94×10^{-7} M were recorded at two excitation wavelengths (λ_{ex} 470 nm and λ_{ex} 580 nm to excite both the neutral and anion species, respectively) at the pH range from 4.08 to 8.95. We observed

that the fluorescence close to the neutral pH was present in a sufficient extent. The dependence of the fluorescence intensity of our compound on the pH value (Figure 20) is presented by the emission spectra. The position of the maximum of the emission spectra ($\lambda_{\text{max em}}$) is slightly shifted to the right and raised to around 602 nm. High pH and polarity of the medium may have led to a shift. Deviations can also be the result of a very intense fluorescence of our compound at high pH.

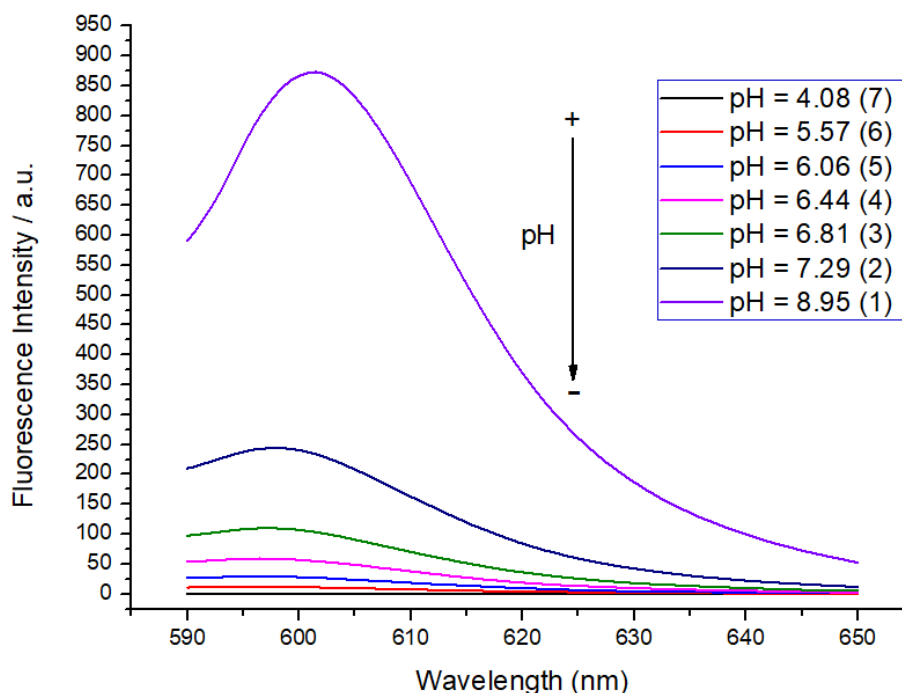


Figure 20: Steady-state emission spectra of **2-Me-4OMe-TM**.

As foreseen, the two different emission spectral profiles, corresponding to the two prototropic forms are presented in the Figure 21. These are the neutral and anion form. To minimize the rate of possible ESPT reactions mediated by the presence of a proton donor/acceptor, we used lower concentrations of phosphate buffer (0.005 M). The recovered pK_a value from the emission spectra from the Figure 20 among the neutral and anion species of **2-Me-4OMe-TM** was 7.8. These values are slightly higher than the ones obtained from the absorption spectra, which were 7.3. But still, the values are very similar, within the range of suitable pK_a for the use of a compound as a fluorescent marker.

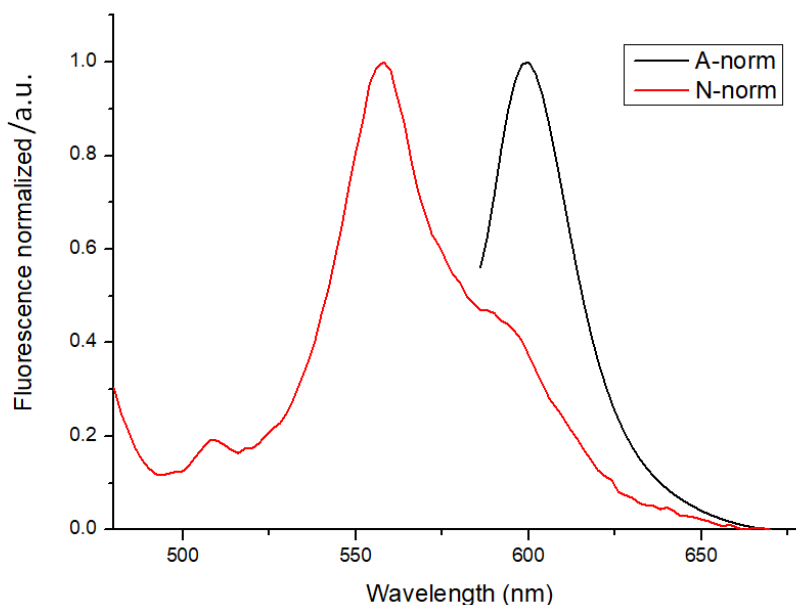


Figure 21: Normalized fluorescence spectral profiles of the two prototropic forms of **2-Me-4OMe-TM**: **anion** (black) and **neutral** (red).

By comparing the emission (Figure 20) to the absorption (Figure 16) spectra it can be noticed that a Stokes shift has taken place. The emission spectra shifted to the longer wavelengths with a length amounting to about 19 nm, which is favorable for this compound as a fluorophore. In the case of absorbance, a shoulder appears which, however, was not visible in the emission spectra.

4.3.1 Produced ESPT reaction

Test solutions of **2-Me-4OMe-TM** of 7.94×10^{-7} M were prepared at different pH values with phosphate buffer at the concentration of 0.7 M, which is high enough to ensure that ESPT reaction will occur in the excited-state. According to the absorption maxima obtained from the absorption spectra presented in Figure 16, steady-state fluorescence spectra were obtained so that we excited the neutral form (470 nm), both species in equilibrium (530 nm) and preferably the anion (580 nm) (Figure 22). Even in these emission spectra a slight shift of the emission maximum to the right is noticeable.

To obtain the value of pK_a^* (pK_a of the proton transfer reaction in the excited-state) by steady-state fluorescence spectra, it is necessary to make a titration curve, in which the normalized intensity maximum is compared with the maximum absorbance at each pH, in order to counterbalance the influence of the steady-state conditions against pH. In this way, we can normalize the absorption of the solutions at different pH values, since not all absorb

equally with the excitation wavelengths used. Thus, by performing an overall adjustment to the experimental data of the three excitation wavelengths, a pK_a^* value of 6.56 ± 0.10 was obtained. pK_a^* is lower than the previously obtained values in the ground-state, which were 7.8 and 7.3. In general, for xanthene derivatives (such as our compound), pK_a and pK_a^* are usually very similar (without large variations between the values). The great importance of knowing the pK_a and pK_a^* , is to predict the behavior of the compound (both in the ground- and excited-state) and to be able to use this information to obtain the kinetic constants that we have studied. All three values are within the range of appropriate values for the use of the compound as a fluorescent marker.

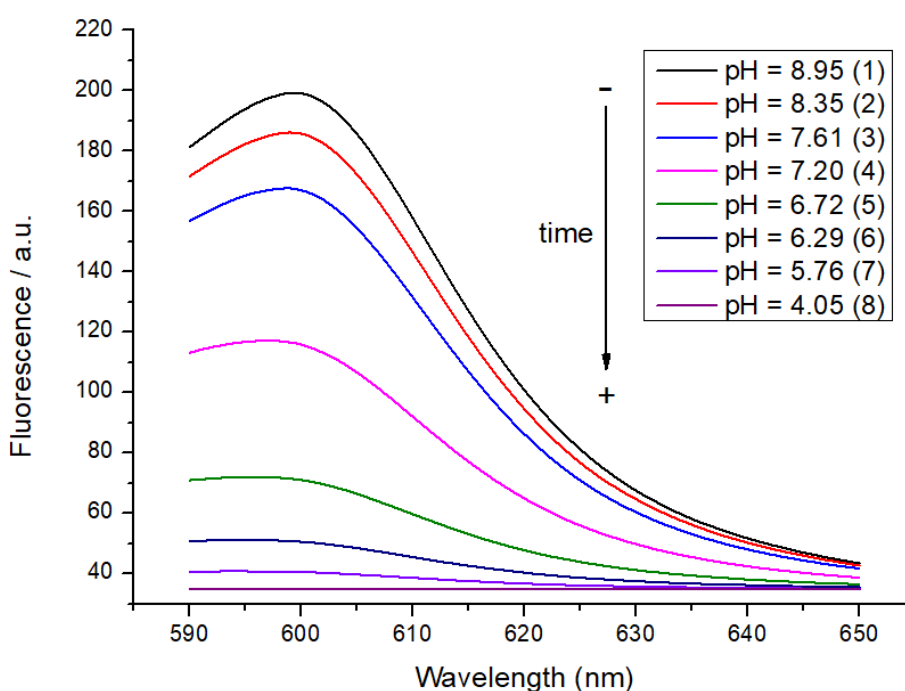


Figure 22: Steady-state emission spectra of **2-Me-4OMe-TM** obtained for the calculation of pK_a^* value.

4.4 TRES

Fluorescence spectra observed at distinct times during the fluorescence decay (TRES) can provide detailed information about the two-state system. We performed TRES with decay traces which were collected from aqueous solutions of **2-Me-4OMe-TM** of 7.94×10^{-7} M in 0.7 M phosphate buffer and at six pH values in the range from 5.59 to 8.95, all the while using the excitation wavelength of 530 nm to preferentially excite the anionic species. Emission in the wavelength range 550-650 nm was recorded in 5 nm steps. The complete data matrix was composed of 231 decay traces and we can describe it by a three-

dimensional surface, $I(\lambda_{\text{ex}}, \lambda_{\text{em}}, t)$, that represents the fluorescence intensity at all excitation and emission wavelengths and times during the fluorescence decay. All of the decay traces could be adjusted using biexponential functions with the exception of one sample, which was adjusted monoexponentially.

Figure 23 shows the TRES generated at pH 7.30 (we chose the pH near to the physiological values, again due to potential use in living cells) and $\lambda_{\text{ex}} = 530$ nm. The TRES are represented at different times after the excitation pulse in the range of 0-4 ns by the normalized emission spectra.

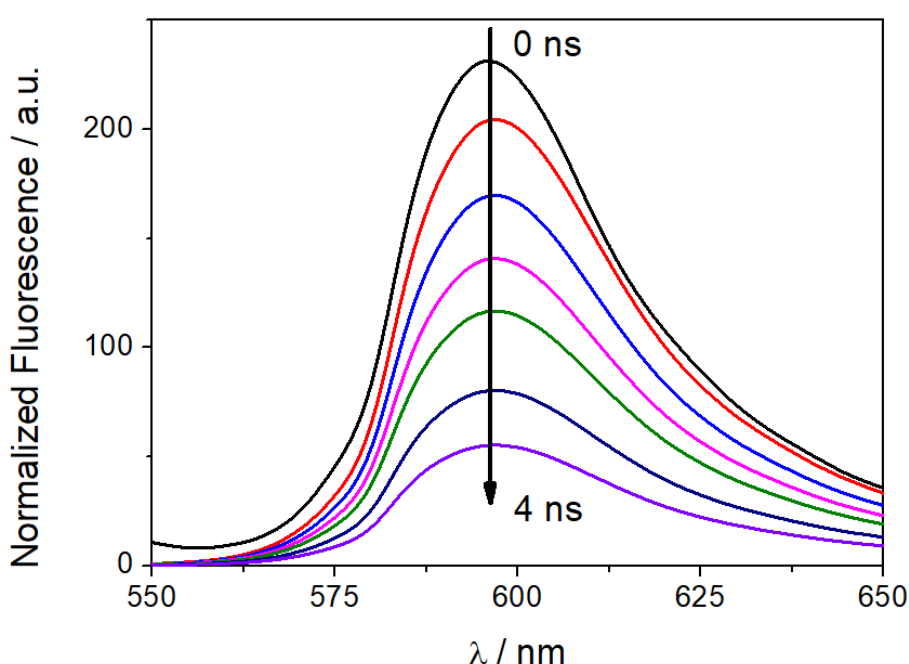


Figure 23: Normalized emission spectra observed at different times after the excitation pulse are shown ($\lambda_{\text{ex}} 530$ nm).

TRES experiments during the excited-state demonstrated a preferred conversion of the anion form to the almost non-fluorescent neutral form which exhibited an emission maximum around 598 nm. In comparison with previous emission spectra from Figure 20 and 22, $\lambda_{\text{max em}}$ occurs at slightly shorter wavelength. Figure 23 indicates that buffer-mediated protonation of the anion form is the main process, with the experimental conditions used (using the $\lambda_{\text{ex}} = 530$ nm). This happened because we were exciting preferentially the anion form. Thus, in the excited-state the predominant specie is the anion, so the species are not in equilibrium anymore. Therefore, the spectra profile at a shorter time after the pulse reflects a large amount of the anion species. By increasing emission

time, the spectral profile was gradually purple-shifted, thus reflecting the successive greater abundance of the neutral species.

If we were to change the conditions and excite the neutral form preferentially, the neutral form would convert into anionic. In any case, we observe the same, the ESPT reaction mediated by phosphate buffer. We preferred to use conditions, using the $\lambda_{\text{ex}} = 530$ nm, since the neutral form is almost non-fluorescent and it would be very difficult to obtain the spectra. Thus, we got an appropriate result, indicating that the emission is decreasing over time. Decay times of fluorescence depend on both the pH and buffer concentration.

4.5 Kinetic and spectral parameters of the ESPT reaction

As to provide a detailed portrayal of the ESPT reaction, which was mediated by the phosphate buffer, we collected the following fluorescence decay surface: pH range from 4.07 to 9.07, and different C^{B} (0, 200, 400 and 700 mM) as a function of λ_{em} (598 nm), with λ_{ex} of 440 and 530 nm and of **2-Me-4OMe-TM** of 7.94×10^{-7} M (Figure 24).

What was interesting as a result is, when added in appropriate concentrations of proton donor/acceptor (phosphate buffer), the ESPT reaction caused changes of the fluorescence decay times, revealing a sensitive decay time in the order of nanoseconds that is dependent on both pH and buffer concentration, while the second decay time was in the sub-nanosecond order (represented by blank spaces in the Figure 24). Since the almost monoexponential fluorescence decay time is suitable for FLIM analysis, we have evaluated the ability of **2-Me-4OMe-TM** dye to assess the concentration of appropriate proton donor/acceptor in samples, simulating the intracellular environment, and inside living cells.

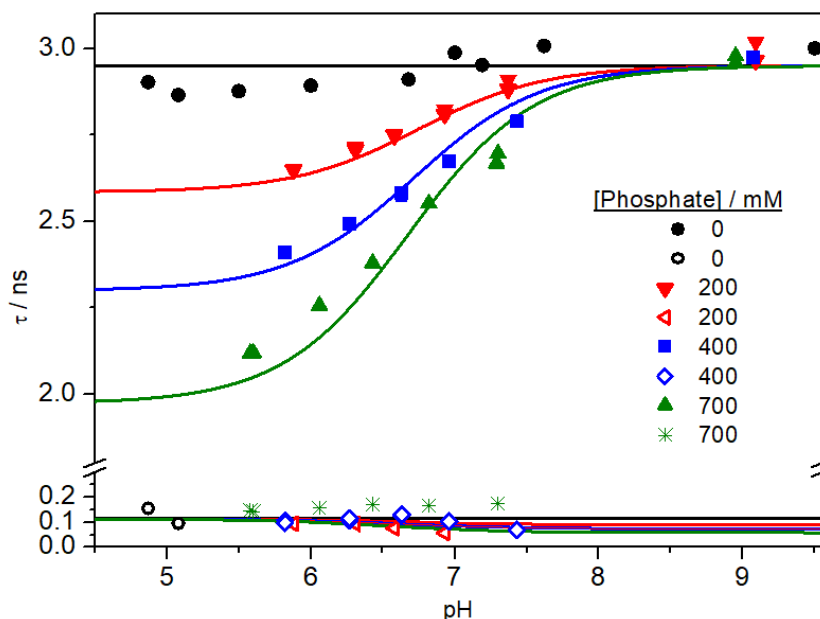


Figure 24: Global fitting (solid lines) of the theoretical equations (eq. 13, 14, 15, 16) to the decay times at different buffer concentrations (0, 200, 400 and 700 mM) and pH values. Note the change in scale between the two sections of the ordinate axis.

Once experimental evidence of the photophysical two-excited-state system was obtained, a multi-dimensional fluorescence decay surface was used to determine the kinetic parameters of the system in the excited-state by using the equations 13, 14, 15, 16. Recovered decay times were fit to equations in order to obtain the kinetic constants of the proton transfer reaction in the excited-state.

The relative obtained values of the rate constants were k_{21}^B ($1.19 \times 10^{10} \text{ s}^{-1}$) and k_{12}^B ($2.40 \times 10^8 \text{ s}^{-1}$). The rate constants' values clearly show the much faster deactivation of the neutral form, which is approximately two orders of magnitude more rapid than the anion deactivation, causing the fluorescence being dominated by the anion emission.

Figure 25 shows the reactions involved in the ESPT model for the two species of **2-Me-4OMe-TM** presented at near-neutral pH. Species **1** and **2** correspond to the neutral and anionic forms of **2-Me-4OMe-TM**, respectively. When excitation by a fast pulse of light is carried out, the excited-state species, **1*** and **2*** are generated (20).

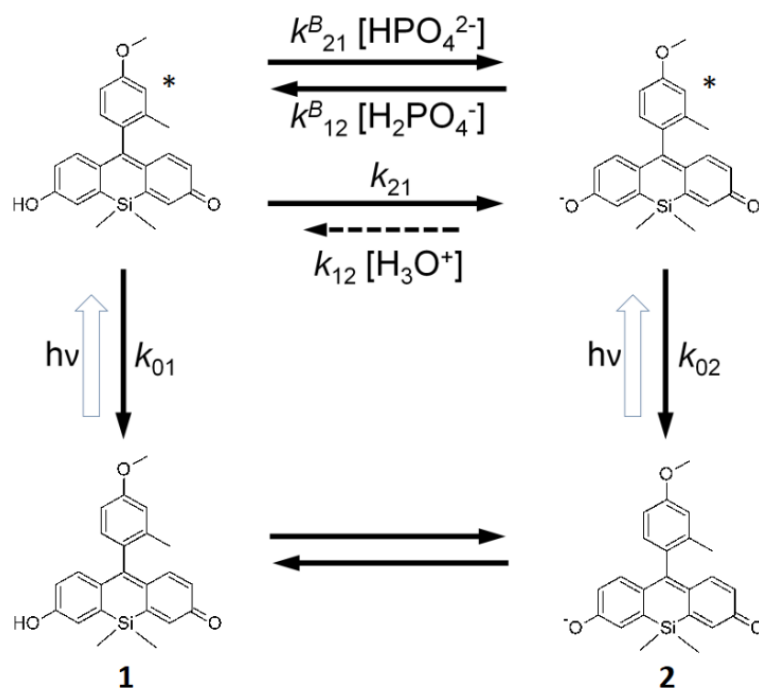


Figure 25: Ground- and excited-state proton-transfer reactions represented by the kinetic model of aqueous **2-Me-4OMe-TM** in phosphate buffer.

4.6 FLIM

Owing to the previous findings and almost monoexponential fluorescence decays of our marker, the compound represented the potential use in cells and the application of the FLIM technique. Its ability to dissolve in water as well as membrane permeability are important properties for a fluorophore that could be functioning inside live cells. **2-Me-4OMe-TM** was applied to DMEM first and then inside cells. The results suggest spontaneous, fast and good membrane penetration without a need for any external molecular assistance. It was freely soluble in aqueous media.

4.6.1 FLIM - biomimetic media DMEM

Intracellular environment could affect the response of our compound. For this purpose we tested the capability of the dye to estimate the concentration of phosphate in solutions, which mimics the cytoplasm firstly by using DMEM media, as a simulator for the cell interior. We excited both, anion (λ_{ex} 530 nm) and neutral (λ_{ex} 470 nm) form of **2-Me-4OMe-TM**. The solutions were stored in a cool and dark place when not in use as to avoid possible deterioration by light and heat. Prepared solutions were plated onto the surface of a microscope glass slide, and recording of the confocal images was implemented by FLIM.

FLIM images are shown after application of an arbitrary colour scale to the recovered fluorescence decay times. From the recovered images it can be observed that the phosphate-response of our compound has good maintenance in these crowded solutions. The results are acceptable, even advantageous as the differences in the phosphate concentrations in the media were clearly noticed despite the complexity of the matrix. It can also be observed, that by increasing the concentration of phosphate buffer, the lifetime of our fluorophore in the DMEM medium rises. (Figure 26, Figure 27) (29).

Pi are the different concentrations of phosphate buffer added to the samples and the color difference observed from the images suggests, that the lifetime of fluorescence of our compound increases when increasing the phosphate concentration. This change in fluorescence intensity is certainly advantageous. The red color illustrates longer lifetimes of our fluorescent compound while the blue color (no phosphate added) signals shorter fluorescence lifetimes. By increasing the concentration of phosphate, the decay time and fluorescence lifetime of our dye have prolonged.

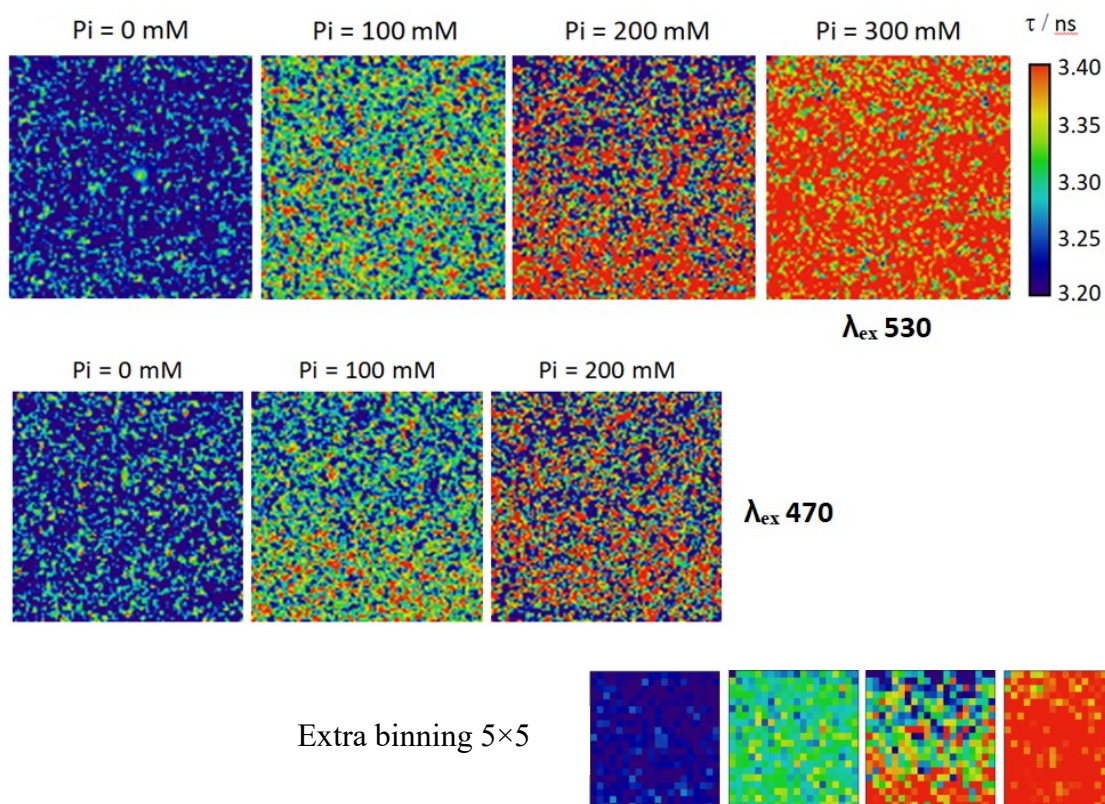


Figure 26: FLIM images of 1×10^{-7} M 2-Me-4OMe-TM in DMEM in 20 mM TRIS buffer, at pH 7.35 and with changing phosphate concentrations in the range of 0 to 300 mM (Pi).

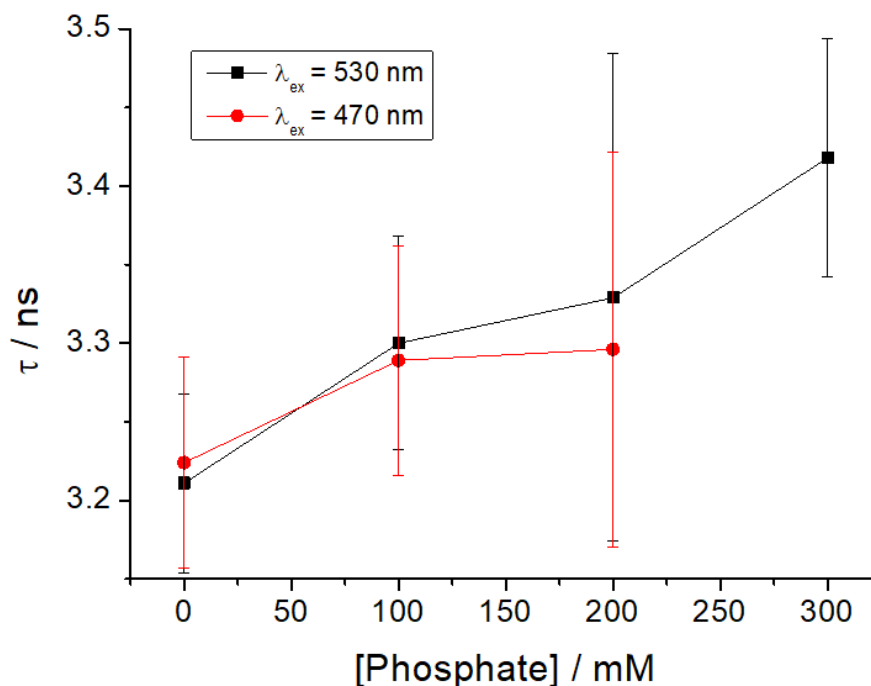


Figure 27: Average decay time (dot) of 1×10^{-7} M **2-Me-4OMe-TM** in DMEM in 20 mM TRIS buffer, at pH 7.35 and with changing phosphate concentrations in the range of 0 to 300 mM obtained from FLIM images and recovered lifetime (line) from the kinetic constants. Red - neutral, black - anion. Scale bars represent the standard deviation.

4.6.2 FLIM - HEK 293 cells

The temporal behavior of the **2-Me-4OMe-TM** fluorescence emission in the intracellular medium and the effect of different concentrations of phosphate ions is an interesting field of observance, therefore we tested our compound by using FLIM in cells, at different differentiation times and by exciting the anion form of the compound (λ_{ex} 530 nm). Good diffusion of our compound and the phosphate anions through the cell membrane was observed. The increase in fluorescence intensity was noticed which reconfirms the ability of **2-Me-4OMe-TM** to detect phosphate concentrations. Changes in fluorescence lifetime, which is longer when the phosphate concentration is increased, enable its behaviour as a potential phosphate concentration sensor. A fairly accurate observation of the phosphate concentration inside the HEK 293 cells and their changes was possible with the employment of a color scale. The accumulation of the compound inside the cytosol was efficient (Figure 28, Figure 29, Figure 30) (36).

PBS (phosphate-buffered saline) was used as a buffer, substance dilution and cell rinsing media. It is isotonic and non-toxic to most cells. Again, as shown by DMEM media, the results are consistent with previous findings, so the red color from the images illustrates

longer lifetimes of our fluorescent compound and the blue color (with no colorant added) signals shorter fluorescence lifetimes. The change in the color scale is linked to the increase of the concentration of phosphate. Two lines of images represent the same; we added two different backgrounds for easier observation and analysis (Figure 28).

If we observe the figure 29, the red colored histogram shows really short fluorescence lifetimes, due to the lack of dye (there is no added dye to the cells). By increasing the phosphate concentration and adding the dye, the fluorescence is extended, which is shown by the shift of histograms to the right, towards the pink histogram, therefore representing the longest lifetime of fluorescence (at the highest concentration of phosphate added). Figure 30 represents average decay time (dot) and recovered lifetime (line) of the compound in cells. Both obtained parameters indicate the change in the decay times and lifetimes of the compound, which rise with the higher concentration of phosphate.

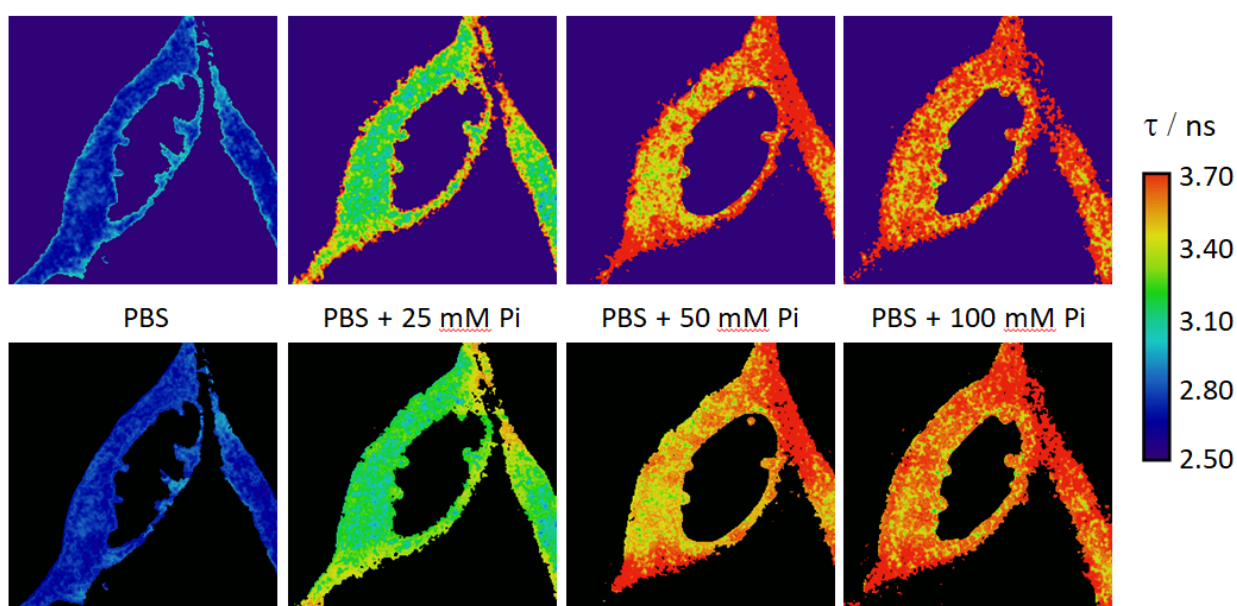


Figure 28: FLIM images of 4×10^{-7} M 2-Me-4OMe-TM in the cytoplasm of HEK 293 cells, treated with different phosphate concentrations.

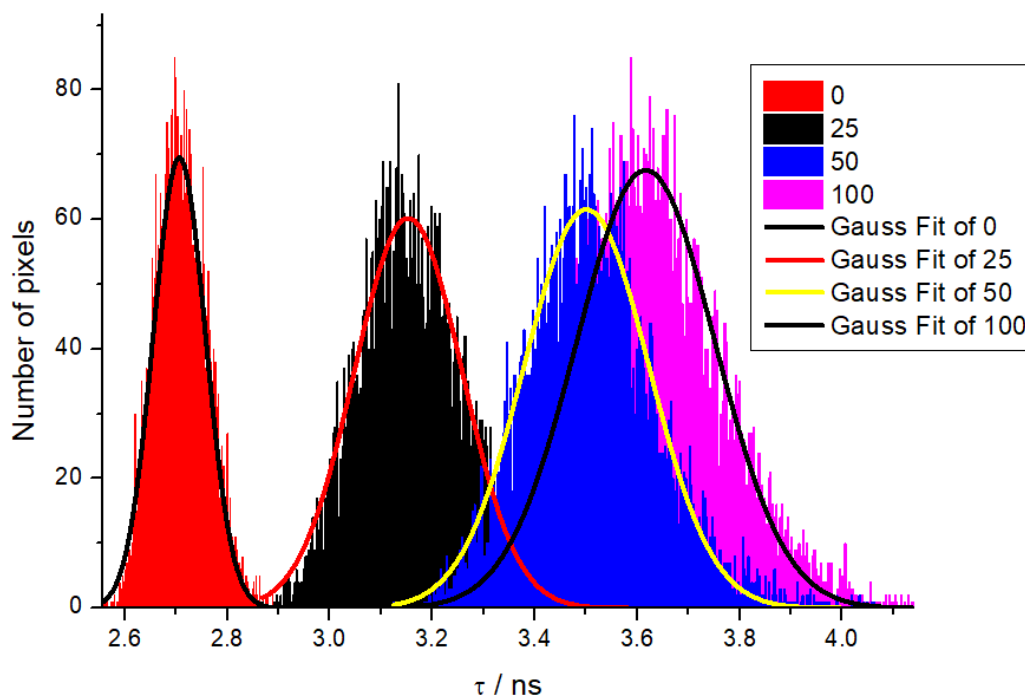


Figure 29: Histograms of lifetimes recovered from Figure 28.

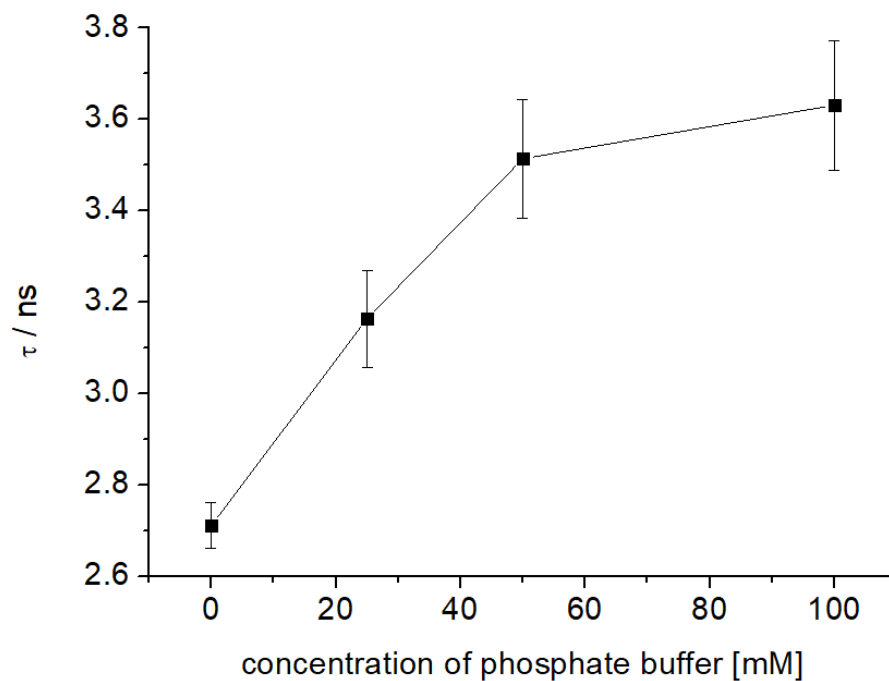
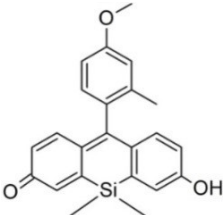


Figure 30: HEK 293 cells, treated with different concentrations of phosphate and the changes in the decay time of the fluorescence are presented in the graph. Average decay time (dot) and recovered lifetime (line).

5 CONCLUSION

The aim of this thesis was to identify the photophysical characteristics of the new silyl-xanthene derivative, **2-Me-4OMe-TM**. From the experimental results, the following conclusions have been obtained:

Table 1: 2-Me-4OMe-TM structure and the obtained photophysical parameters.

2-Me-4OMe-TM	
Solubility	Freely soluble in water
Observed species	Neutral, anion
p <i>K</i> _a	7.3, 7.8
p <i>K</i> _a [*]	6.56
λ _{max abs anion}	583 nm
λ _{max abs neutral}	480 nm
λ _{isob point}	524 nm
λ _{ex}	440 or 470 nm (neutral), 530 or 580 nm (anion)
λ _{max em}	602 nm
Stokes shift	✓ 19 nm
ESPT reaction in excited-state	✓
<i>k</i> ₂₁ ^B	1.19×10 ¹⁰ s ⁻¹
<i>k</i> ₁₂ ^B	2.40×10 ⁸ s ⁻¹

- The absorption and emission spectra at steady-state showed two spectroscopically distinguishable species (anion and neutral form) around the physiological pH, which are converted into one another as the pH varies.
- Absorption spectra are narrow, with well-visible absorption maximum and a clearly visible isosbestic point. The emission maximum were slightly shifted to the right at high pH values, which is not ideal, but still the result is satisfactory.

- We determined the acidity constants of our dye at near-neutral pH, both in the ground- and in the excited-state. Based on the values obtained, it can be concluded that our compound has pK_a values in the range of interesting pH values for potential application in cells at near-neutral pH.
- An ESPT reaction was observed between the neutral and the anion species of our compound in aqueous solutions at near-neutral pH (mediated by the presence of phosphate buffer).
- The results from TRES indicate that the buffer-mediated protonation of the anion form is the main process, occurring during the ESPT reaction and the anion has a strong fluorescence, which is beneficial.
- Almost monoexponential fluorescence decays observed by FLIM indicate on the potential use of the compound in cells.
- Finally due to the good cell penetration of our dye and obtained photophysical parameters, we determined that **2-Me-4OMe-TM** could be used as a potential real-time phosphate intracellular marker in grown cells by using technique FLIM. Our compound is suitable for labeling more basic cell cultures with the pK_a value around near-neutral pH.

6 REFERENCES

1. Douglas A. Skoog, F. James Holler, Timothy A. Nieman: Principles of Instrumental Analysis (Fifth edition), Hartcours Brace & Company, Florida, 1998: 115-142, 300-328.
2. Lobnik, A.: Skripta za vaje pri predmetu Okoljska analitika, Univerza v Mariboru, Fakulteta za strojništvo, Tiskarna tehniških fakultet, Maribor, 2010: 2-4.
3. <http://www.physicsclassroom.com/class/light/Lesson-2/Light-Absorption,-Reflection,-and-Transmission>. (15.7.2017)
4. <http://goldbook.iupac.org/html/B/B00626.html>. (16.7.2017)
5. <http://life.nthu.edu.tw/~labcyjw/BioPhyChem/Spectroscopy/beerslaw.htm>. (17.7.2017)
6. Petra Hohler: Master's thesis - Evaluation of pH dependent photo-physical properties of selected rhodamine derivatives. University of Ljubljana, Faculty of Pharmacy, Ljubljana, 2014: 3-5.
7. <http://goldbook.iupac.org/html/I/I03310.html>. (20.7.2017)
8. Crovetto L., Orte A., Paredes J. M., Resa S., Valverde J., Castello F., Miguel D., Cuerva J. M., Talavera E. M., Alvarez-Pez J. M.: Photophysics of a Live-Cell-Marker, Red Silicon-Substituted Xanthene Dye. *J Phys Chem A*, 2015; 119: 10854-62.
9. Javier Valverde Pozo: Master's thesis - Cálculo del pKa de silil-xantenonas mediante espectroscopia de absorción y de emisión. University of Granada, Faculty of Pharmacy, Granada, Spain, 2015: 20.
10. https://en.wikipedia.org/wiki/Isosbestic_point#/media/File:Bromocresol_green_spectrum.png. (25.7.2017)
11. Darinka Brodnjak Vončina: Analizna kemija II (zbrano gradivo), Univerza v Mariboru, Fakulteta za kemijo in kemijsko tehnologijo, Maribor, maj 2006: 14-21.
12. Michael L. Bishop, Edward P. Fody, Larry E. Schoeff: *Clinical Chemistry: Principles, Techniques, Correlations*, Lippincott Williams & Wilkins, Philadelphia, 2010: 130-140.

13. <http://sites.cord.edu/chem-330-lab-manual/experiments/uv-vis>. (25.7.2017)
14. Joseph R., Lakowicz: Principles of Fluorescence Spectroscopy, 3rd ed., Springer Science + Business Media, LLC, New York, 2006: 1-8.
15. Peter Jomo Walla: Modern Biophysical Chemistry, WILEY-VCH Verlag GmbH & Co. KGaA, Weinheim, 2009: 61-100.
16. Peter Atkins, Julio de Paula: Physical Chemistry, W.H. Freeman and Company, USA, 2010: 445-520.
17. Ruedas-Rama M. J., Alvarez-Pez J. M., Crovetto L., Paredes J. M., Orte A.: FLIM Strategies for Intracellular Sensing - Fluorescence Lifetime Imaging as a Tool to Quantify Analytes of Interest. © Springer International Publishing Switzerland, 2014; 15: 191–224.
18. Paredes J. M., Crovetto L., Rios R., Orte A., Alvarez-Pez J. M., Talavera E. M.: Tuned lifetime, at the ensemble and single molecule level, of a xanthenic fluorescent dye by means of a buffer-mediated excited-state proton exchange reaction. Phys Chem Chem Phys, 2009; 11: 5400-5407.
19. http://iopscience.iop.org/journal/2050-6120/page/Excited_state_proton_transfer. (5.8.2017)
20. Virginia Puente Muñoz: PhD Thesis - New fluorescent dyes for biologically relevant analytes detection. Design, synthesis and photophysical characterization, application in biological media. University of Granada, Faculty of Pharmacy, Granada, Spain, 2017.
21. Alvarez-Pez J. M., Ballesteros L., Talavera E., Yguerabide J.: Fluorescein Excited-State Proton Exchange Reactions: Nanosecond Emission Kinetics and Correlation with Steady-State Fluorescence Intensity. J. Phys. Chem. A., 2001; 105 (26): 6320–6332.
22. https://www.google.si/search?client=firefox-b&dcr=0&biw=1467&bih=725&tbm=isch&sa=1&q=fluorescein+structures&oq=fluorescein+structures&gs_l=psy-ab.3...109954.113324.0.113585.11.11.0.0.0.168.1341.0j11.11.0....0...1.1.64.psy-ab..0.10.1237...0i19k1j0i8i30i19k1j0i30i19k1.50XjxLRha_8#imgcr=8au8a2BEP2sT7M: (10.8.2017)

23. Resa S., Orte A., Miguel D., Paredes J. M., Puente-Muñoz V., Salto R., Giron M. D., Ruedas-Rama M. J., Cuerva J. M., Alvarez-Pez J. M., Crovetto L.: New Dual Fluorescent Probe for Simultaneous Biothiol and Phosphate Bioimaging. *Chem. Eur. J.*, 2015; 21: 14772-14779.
24. Crovetto L., Orte A., Talavera E. M., Alvarez-Pez J. M.: Global Compartmental Analysis of the Excited-State Reaction between Fluorescein and (\pm)-N-Acetyl Aspartic Acid. *J. Phys. Chem. B*, 2004; 108 (19): 6082–6092.
25. <http://www.labcompare.com/10-Featured-Articles/171083-Spectrofluorometers-Tools-for-Measuring-Fluorescence-Signature/>. (10.8.2017)
26. <https://www.picoquant.com/applications/category/life-science/time-resolved-fluorescence>. (11.8.2017)
27. http://www.horiba.com/fileadmin/uploads/Scientific/Documents/Fluorescence/Tech_Note4_-_TRES-DAS.pdf. (11.8.2017)
28. <https://www.picoquant.com/products/category/fluorescence-microscopes/microtime-200-time-resolved-confocal-fluorescence-microscope-with-unique-single-molecule-sensitivity#papers>. (11.8.2017)
29. Paredes J. M., Giron M. D., Ruedas-Rama M. J., Orte A., Crovetto L., Talavera E. M., Salto R., Alvarez-Pez J. M.: Real-time phosphate sensing in living cells using fluorescence lifetime imaging microscopy (FLIM). *J Phys Chem B.*, 2013; 117: 8143-9.
30. Best, Q. A., et al.: pH-Dependent Si-Fluorescein Hypochlorous Acid Fluorescent Probe: Spirocycle Ring-Opening and Excess Hypochlorous Acid-Induced Chlorination. *J. Am. Chem. Soc.*, 2013; 135: 13365-13370.
31. Juan Manuel Cuerva Carvajal (organometallic chemistry and molecular electronics), on the Department of Organic Chemistry at the Faculty of Science of the University of Granada, Spain. Synthesis of 2-Me-4OMe-TM, 2015.
32. A. Q. Sattenapally, N. Dyer, D. J. Scott, C. N. McCarroll, M. E. J. Best et al.: *Am. Chem. Soc.*, 2013; 135: 13365-13370.

33. <http://www.optoscient.com/cat2.php?id=107>. (15.8.2017)
34. <https://fiji.sc/>. (15.8.2017)
35. Crovetto L., Orte A., Paredes J. M., Resa S., Valverde J., Castello F., Miguel D., Cuerva J. M., Talavera E. M., Alvarez-Pez J. M.: Supporting information - Photophysics of a Live-Cell-Marker, Red Silicon-Substituted Xanthene Dye. *J Phys Chem A*, 2015; 119: 10854-62.
36. Martínez-Peragón A., Miguel D., Orte A., Mota A. J., Ruedas-Rama M. J., Justicia J., Alvarez-Pez J. M., Cuerva J. M., Crovetto L.: Rational design of a new fluorescent 'ON/OFF' xanthene dye for phosphate detection in live cells. *Org Biomol Chem*, 2014; 12: 6432-9.
37. <http://www.sigmaaldrich.com/life-science/biochemicals/biochemical-products.html?TablePage=17902163>. (16.8.2017)
38. <http://www.sigmaaldrich.com/life-science/cell-biology/detection/fluorescence-lifetime-measurement.html>. (16.8.2017)